Aus der AG Immunphysiologie, Institut für Physiologie und Pathophysiologie

des Fachbereichs Medizin der Philipps-Universität Marburg

Unter der Leitung von Prof. Dr. A. del Rey

Metabolic changes in the brain as consequence of IL-1-induced hypoglycemia: involvement of MyD88

Inaugural-Dissertation zur Erlangung des Doktorgrades

der Humanmedizin

dem Fachbereich Medizin der Philipps-Universität vorgelegt von

Moritz Verdenhalven

Geboren in Bad Soden am Taunus

MARBURG AN DER LAHN 2015

Angenommen vom Fachbereich Medizin der Philipps-Universität Marburg
am: 09.11.2015
Gedruckt mit Genehmigung des Fachbereichs.
Dekan: Prof. Dr. med. Helmut Schäfer
Referent: Prof. Dr.phil. Adriana del Rey
1. Korreferent: Prof. Dr. med. Richard Dodel

Table of Contents

ABSTRACT **6**

ZUSAMMENFASSUNG **7**

1 INTRODUCTION **8**

1.1 General background **8**

1.2 The IL-1 family **8**

1.2.1 IL-1 receptors and signalling 9

1.2.2 MyD88 10

1.2.3 IL-1β and the brain 12

1.2.4 IL-1β and energy metabolism 15

1.3 Corticosterone **17**

1.4 Astrocyte-Neuron-Lactate-Shuttle **18**

1.5 Central glucose-regulation **19**

1.6 Magnetic resonance spectroscopy **20**

1.6.1 Operation principle 20

1.6.2 Metabolites 21

1.7 Aims and objectives **23**

2 MATERIAL AND METHODS **24**

2.1 Animals **24**

2.2 Material **24**

2.3 Methods **29**

2.3.1 Gentoyping 29

2.3.2 Injection 29

2.3.3 Blood collection 29

2.3.4 Glucose determination 30
2.3.5 Corticosterone determination 30
2.3.6 Magnetic resonance spectroscopy 30

2.4 Substances and Vehicles 32

2.5 Experimental setups 33
2.5.1 Effect of IL-1β injection on blood glucose and stimulation of the HPA-axis 33
2.5.2 Pharmacological inhibition of MyD88 signalling 34
2.5.3 Magnetic resonance spectra of IL-1β-, insulin- and vehicle- injected mice 35
2.5.4 Influence of isoflurane on insulin-induced hypoglycemia 36

2.6 Statistical analyses 37

3 RESULTS 38

3.1 IL-1β effects on glucose and corticosterone blood levels are MyD88-dependent 38
3.1.1 No effect of IL-1β on blood glucose levels in MyD88 KO mice 38
3.1.2 No effect of IL-1β on corticosterone blood levels in MyD88 KO mice .. 41

3.2 Pharmacological inhibition of MyD88 signalling does not influence IL-1β-induced hypoglycemia, but affects basal glucose levels 43
3.2.1 IMG2005 injection does not affect IL-6 levels 43
3.2.2 IMG2005 affects basal glucose concentrations but not IL-1β-induced hypoglycemia 44
3.2.3 IMG2005 does not influence plasma corticosterone levels 45

***3.3* IL-1β injection affects brain energy metabolism 46**
3.3.1 Changes in blood glucose concentrations after insulin and vehicle injection but not after IL-1β injection during the MRS procedure 46
3.3.2 Plasma corticosterone concentrations increase during the MRS scan 49
3.3.3 Differences in brain metabolites between IL-1β-, Insulin- and vehicle-injected animals 51

4 DISCUSSION 56

4.1 IL-1β-induced hypoglycemia and the stimulation of the HPA-axis depend on MyD88-mediatied signalling 56

4.2 Changes in glucose and corticosterone levels during MRS 57

4.3 IL-1β affects brain energy metabolism: differences with the effects of insulin 59

4.4 Conclusion and perspectives 61

5 REFERENCES 63

6 APPENDIX 75

ABSTRACT

IL-1β induces a profound and long-lasting hypoglycemia in C57BL/6J mice (wild type, WT) and resets glucose homeostasis at central levels. Intracerebroventricular (i.c.v.) injection of IL-1 at a dose that has no effect when injected intraperitoneally (i.p.), induces hypoglycemia, even after a glucose load. Interestingly, IL-1 also increases corticosterone plasma levels, although this effect is of shorter duration than hypoglycemia.

Myeloid-differentiation factor 88 (MyD88) is a central adaptor molecule involved in IL-1 signalling, but MyD88-independent IL-1-signalling pathways have also been described. The first part of this work investigated if IL-1β-induced hypoglycemia and the increase in glucocorticoid levels are MyD88-dependent by using two approaches: a) administration of IL-1β into MyD88 knockout (MyD88KO) mice; and b) pharmacological inhibition of MyD88 in WT mice prior to IL-1β injection. No changes in glucose and corticosterone blood levels were detected in MyD88KO mice after IL-1β injection as compared to WT mice. Administration of the MyD88 inhibitor to WT mice did not abolish the hypoglycaemic effect of IL-1. Since the inhibitor did not affect IL-1-induced IL-6 production either, it is possible that the concentration used was insufficient. However, a short-lasting hyperglycaemia was observed when the inhibitor was injected alone to WT mice. Particularly the results obtained in MyD88KO mice show that IL-1β-induced hypoglycemia and the increase in corticosterone concentrations depend on this adaptor molecule. The second part of this thesis studied cerebral energy metabolism during IL-1β-induced hypoglycemia, and compared it to the effects of a similar hypoglycemia induced by insulin, and to euglycaemic conditions. *In vivo* cerebral H^1-magnetic resonance spectroscopy (MRS) was used for this purpose. It was found that, as opposite to insulin, the concentrations of lactate, creatine, and *N*-acetyl aspartate, in relation to those of choline, are increased during IL-1β-induced hypoglycemia. These results provide further evidence that IL-1β injected peripherally influences cerebral energy metabolism in parallel to a long-lasting and profound hypoglycemia. Besides its relevance for normal physiology, these results might be important during psychiatric diseases during which impairments of cerebral energy metabolism are observed, but also several immune-derived cytokines are involved.

ZUSAMMENFASSUNG

IL-1β induziert eine tiefe und lang anhaltende Hypoglykämie bei C57BL/6J Mäusen und führt zu einer Neueinstellung des Blutzuckersollwerts im Gehirn. Intrazerebroventrikuläre IL-1-Injektion, in einer Dosis die keinen Effekt hat wenn sie peripher injiziert wird, induziert eine Hypoglykämie, die sich nach Glukosebolusgabe erneut einstellt. Interessanterweise führt IL-1 außerdem zu erhöhten Plasmacorticosteronwerten, auch wenn dieser Effekt kürzer anhält als die Hypoglykämie. Ein zentrales Adapterprotein des IL-1-Rezeptors zur intrazellulären Signaltransduktion ist der Myeloid-differentiation Faktor 88 (MyD88). Es gibt jedoch auch MyD88-unabhängige Signalkaskaden von IL-1. Der erste Teil dieser Arbeit untersucht, ob die von IL-1β hervorgerufene Hypoglykämie und die erhöhten Corticosteronwerte abhängig von MyD88 sind. Hierfür wurden zwei verschiedene Anätze gewählt: a) IL-1β-Injektion in MyD88 knockout Mäuse; und b) Verabreichen eines pharmakologischen MyD88-Inhibotrs vor IL-1β-Injektion. Im Vergleich zu WT Mäusen entwickelten MyD88KO Mäuse weder eine Hypoglykämie noch erhöhte Corticosteronwerte. Die Injektion des Inhibitors verhinderte hingegen nicht die Entwicklung einer IL-1β induzierten Hypoglykämie, führte aber zu einem kurzfristigen Anstieg der Blutzuckerwerte. Da außerdem die Produktion von IL-6 durch den Inhibitor nicht beeinflusst wurde, ist davon auszugehen, dass die verabreichte Konzentration zu gering war. Vor Allem die Versuche mit den MyD88KO Mäusen zeigen, dass MyD88 notwendig ist, um eine IL1-induzierte Hypoglykämie entwickeln zu können. Im zweiten Teil der Arbeit wurde der Energiestoffwechsel im Gehirn während IL-1 induzierter Hypoglykämie untersucht und mit Insulin induzierter Hypoglykämie und Euglykämie verglichen. Hierfür wurden *in vivo* H^1 Magnetresonanzspektroskopien (MRS) durchgeführt. Die Konzentrationen von Kreatin, Laktat und *N*-Acetyl Aspartat im Vergleich zur Cholinkonzentration waren bei IL-1 induzierter Hypoglykämie höher als bei Insulin-induzierter Hypoglykämie oder Euglykämie. Dies ist ein weiterer Hinweis darauf, dass peripher injiziertes IL-1 den zerebralen Energiestoffwechsel so beeinflusst, dass es zu einer charakteristischen Hypoglykämie kommt. Abgesehen von der physiologischen Relevanz könnten diese Prozesse auch eine Rolle bei psychiatrischen Erkrankungen führen, bei denen es zu Veränderungen des zerebralen Energiestoffwechsels kommt und Cytokine involviert sind.

1 INTRODUCTION

1.1 General background

Interleukin-1 (IL-1) was originally described as leukocyte-derived factor able to induce fever (Dinarello, 2010). Experiments with purified supernatant of activated leukocytes showed various different properties of the so-called human leukocytic pyrogen such as induction of hepatic acute-phase proteins, activation of lymphocytes and induction of prostaglandin synthesis (Dinarello, 2010). The cloning of IL-1 finally allowed to prove that the above described effects were all induced by a single molecule, and additional effects such as bone marrow stimulation (Smith et al., 1993) and induction of type-1 diabetes (Bendtzen et al., 1986) were described. Another effect of IL-1 is the induction of a profound and long-lasting hypoglycemia and the resetting of glucose homeostasis at central levels (del Rey and Besedovsky, 1987; del Rey and Besedovsky, 1992; del Rey et al., 2006). Even after a glucose load, IL-1β-induced hypoglycemia lasts longer than insulin induced-hypoglycemia. Furthermore, when glucose is injected after IL-1β hypoglycaemic values are quickly regained and maintained for hours (del Rey et al., 2006). This change of set point must take place at cerebral levels and one possibility is that it is caused by a change in energy substrate transport or metabolism in neurons. Magnetic resonance spectroscopy was used in this work to evaluate cerebral energy metabolism under IL-1β-induced hypoglycemia *in vivo*. Furthermore, it was studied whether the myeloid differentiation factor 88 (MyD88), a central downstream protein mediating the IL-1 receptor I (IL-1RI) signalling, is involved in the hypoglycaemic effect of the cytokine.

1.2 The IL-1 family

IL-1β belongs to the IL-1 family consisting of 11 cytokines: IL-1α, IL-1β, IL-1 receptor antagonist (IL-1ra), IL-18, IL-33, IL-36α, IL-36β, IL-36γ, IL-36ra, IL-37 and IL-38. It is considered that these Interleukins originate from the same ancestral gene because they share a large homology in their gene structure and key amino acid structure, so that each protein forms a 12-stranded β-barrel (Dinarello, 1991, 2011; Rupp et al., 1986; Sims and Smith, 2010).

The gene encoding for IL-1α has 10.5 kilobases (kb), whereas the IL-1β gene consists of 7.8 kb. 7 exons of both genes form the mRNA, which is translated to a

Pro-IL-1 protein of 31Kilodalton (kDa) (Dinarello, 1991). In the case of IL-1β, this pro-IL-1-peptide is intracellularly cleaved by Caspase-1 to mature IL-1β of 15 kDA, which is the form finally released (Dinarello, 2005). Pro-IL-1α remains within the cell or at the cell surface. So either pro-IL-1α is released after cell death and then activated, or membrane bound IL-1α gets cleaved by calpain to its soluble form (Dinarello, 1996). Furthermore, pro-IL-1α is able to translocate into the nucleus and act as transcription factor (Dinarello, 2011).

IL-1 was first described as an endogenous pyrogen with the ability to generate fever (Atkins, 1960). It plays a central role in host-defence by activating various cell types such as fibroblasts, thymocytes and B- and T-lymphocytes. Moreover, IL-1 induces the synthesis of other cytokines, such as IL-2 and IL-6 as well as its own production and leads to the expression of different genes, such as Cyclooxygenase-2 (COX-2), inducible NO-Synthetase (iNOS) and acute-phase proteins, and also growth factors, such as platelet derived growth factor (PDGF), nerve growth factor (NGF) and Insulin-like growth factor 1 (IGF-1) (Dinarello, 1996). In addition, IL-1 influences several neuro-endocrine and metabolic pathways.

IL-1ra is a physiologically occurring antagonist of IL-1. It binds to IL-1 receptor type 1 (IL-1RI) but does not lead to heterodimerization (see 1.2.1) which is essential for intracellular signalling (Garlanda et al., 2013).

1.2.1 IL-1 receptors and signalling

There are two subtypes of IL-1 receptors (IL-1R), but only the type 1 receptor transduces an intracellular signal after binding IL-1. The type 2 IL-1 receptor (IL-1RII) lacks an intracellular signalling domain and thus serves as a decoy receptor. IL-1RII, like IL-1ra, contributes to regulate IL-1 effects by binding the free cytokine thus limiting the effects of soluble IL-1 (Dinarello, 2011). IL-1-signalling pathways are complex and include a variety of intracellular kinases, which lead to the activation of nuclear factor kappa B (NF-κB) and activator protein 1 (AP-1). These factors control most of the pro-inflammatory effects induced by IL-1 (Garlanda et al., 2013). Only the signalling pathways essential for this work will be described below. For a detailed review of IL-1 signalling see Weber et al., 2010.

After binding IL-1, the IL-1-IL-1RI complex recruits the IL-1 receptor accessory protein (IL-1RacP), which then binds the myeloid differentiation primary response factor 88 (MyD88) to the intracellular Toll- and IL-1R-like domain (TIR domain,

Figure 1). This TIR domain is common to all Toll-like receptors (TLRs) and the IL-1RI. The recruitment of MyD88 occurs after ligand binding of IL-1RI and all TLRs, with the exception of TLR3 (Akira and Takeda, 2004). MyD88 leads to phosphorylation and activation of several downstream kinases such as IRAK-4, Src and the mitogen-activated kinases (MAPK) (Davis et al., 2006; Kenny and O'Neill, 2008).

Recent evidence showed that IL-1 can also signal via a MyD88-independent mechanism (Davis et al., 2006; Kenny and O'Neill, 2008). Inhibition of MyD88 by a synthetic peptide blocking the TIR domain for MyD88 recruitment leads to IL-1-induced activation of Akt-Kinase via Posphinositol-3 kinase (PI3K). A direct interaction between the p85 subunit of PI3K and the IL-1RI/IL-1RacP complex is described in this publication. The results were confirmed using neurons from MyD88-deficient mice (Davis et al., 2006). Section 1.2.3 describes how the PI3K/Akt pathway elicits neuroprotective effects (Diem et al., 2003; Tsakiri et al., 2008).

IL-1β-induced activation of Src in neurons leads to expression of IL-6 and to an increased activation of NMDA receptors resulting in an augmented Ca^{2+}-influx and increased glutamate- or NMDA-induced cell death. This signalling pathway is MyD88-dependent (Davis et al., 2006; Viviani et al., 2003). Interestingly, IL-1β induces IL-6 expression in glia cells by the “classical” signalling pathway via MyD88, MAPK and NFκB (Parker et al., 2002). Furthermore, higher concentrations of IL-1β are needed to induce IL-6 production in glia as compared to neurons (Tsakiri et al., 2008).

Recently, a splicing variant of IL-1RacP called IL-1RacPb has been described. It signals independently of MyD88 and is expressed in hippocampal neurons but not in astrocytes. RacPb is not only necessary for Src phosphorylation and activation, but it can also induce Src phosphorylation when transfected into astrocytes. Src phosphorylation peaks at low doses of IL-1, corresponding to facilitation of long-term potentiation by IL-1β at physiological cerebral concentrations (Huang et al., 2011).

Moreover, there is evidence of effects of IL-1β that are independent of the IL-1RI. In retinal ganglion cells, IL-1β-induced changes in sodium and potassium fluxes can be observed, which are not blocked by IL-1ra (Diem et al., 2003).

1.2.2 MyD88

MyD88 is the main intracellular adaptor molecule for all receptors belonging to the TLR/IL-1R (TIR) family with the exception of TLR3 (Akira and Takeda, 2004). Even though there are some MyD88-independent signalling pathways, MyD88 is essential for most effects of the TIR family (Oda and Kitano, 2006). TLRs are essential for innate immunity since they recognize pathogen-associated molecular patterns (PAMPs), such as LPS (TLR4), double-stranded RNA (TLR3) or bacterial Flagellin (TLR5) (Akira and Takeda, 2004). Hence TLRs are responsible for the first response of the immune system to intruding bacteria, viruses or parasites (O'Neill and Bowie, 2007). Accordingly, the response to IL-1 or to PAMPs detected by TLRs using MyD88 as adaptor protein is disturbed in MyD88-deficient mice (MyD88 KO mice). This results in an increased susceptibility to gram positive (e.g. Staphylococcus Aureus, Takebuchi et al., 2000), gram negative (e.g. Ehrlichia muris, Koh et al., 2010), parasitic (e.g Toxoplasma gondii, Scanga et al., 2002) or viral (lymphocytic choriomeningitis virus (Zhou et al., 2005)) infections. Increased susceptibility in this case implies increased concentrations of microorganisms in blood and other organs, decreased pro-inflammatory reactions, such as cytokine production and splenomegaly, or increased death rates. As expected, MyD88 KO mice show a hypo-responsiveness to LPS, as evaluated by decreased cytokine production, septic shock and death (Kawai et al., 1999), as well as an impaired IL-1 response resulting in no detectable IL-6 and TNF-α levels in plasma and impaired IL-1-induced T-cell proliferation (Adachi et al., 1998). However, MyD88 KO mice show no obvious abnormalities up to 20 weeks of age as compared to wild type (WT) C57BL/6J mice. There are no differences between MyD88 KO mice and C57BL/6J mice at 16 weeks of age concerning food intake, body weight (b.w.) and locomotor activity, but the same study showed an increase in fasting blood glucose levels in MyD88 KO mice (Hosoi et al., 2010). Raetzsch et al. showed that TLR4 and MyD88 are essential for LPS-induced hypoglycemia (Raetzsch et al., 2009). This might be due to the loss of LPS-induced IL-1 production, which plays a major role in LPS-induced hypoglycemia, as shown by del Rey et al. C57BL/6J mice that received LPS and IL-1ra injected i.p. showed statistically significant higher blood glucose levels than animals that received LPS alone (del Rey et al., 2006).

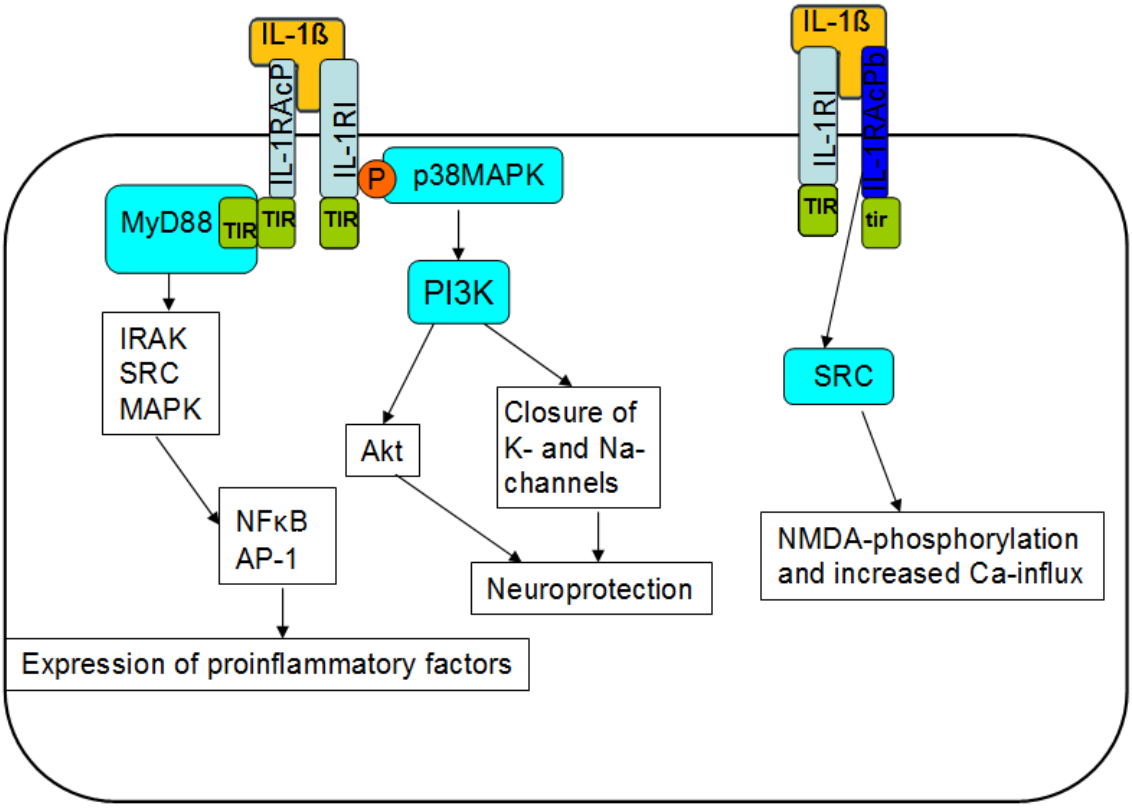

Figure 1 Different mechanisms of IL-1β signalling. IL-1β signals via IL-1RI-RacP complex MyD88-dependently, which leads to activation of NFκB and AP-1 eliciting a pro-inflammatory response. The MyD88-independent pathway of the IL-1RI-RacP complex causes the closure of NA^+- and K^+-channels and neuroprotection via activation of p38 MAP-kinase and PI3-kinase. The signalling of IL-1RAcPb is neuron specific. It activates SRC-kinase leading to phosphorylation of NMDA-receptors and increased Ca^{2+}-influx into the neuron.

1.2.3 IL-1β and the brain

IL-1β influences the brain at different levels. It leads to the activation of the hypothalamus-pituitary-adrenal (HPA) axis, resulting in increased blood levels of ACTH and corticosterone. This effect is not due to IL-1-induced fever or the induction of other cytokines, such as tumor-necrosis-factor (TNF)-α or to T-cell derived cytokines such as IL-2 (Besedovsky et al., 1986) but is exerted directly in the hypothalamus at the level of corticotropin-releasing factor liberating neurons (Berkenbosch et al., 1987; Sapolsky et al., 1987).

IL-1β, together with other cytokines, such as IL-6 and TNF-α, is also involved in a phenomenon called “sickness behaviour”. Sickness behaviour is characterized by malaise, fatigue, anorexia, joint and muscle aches, coldness, fever and a change in the endocrine status (Konsman et al., 2002), which frequently occur in case of

viral or bacterial infections and allows the body an efficient way to combat the intruding microorganisms and to better deal with the infection (Dantzer, 2009).

IL-1 plays a critical role in neuronal injury due to trauma or insult and in neurodegenerative disorders. Application of IL-1 in ischemic areas leads to increased neuronal death, whereas IL-1ra administration decreases neuronal death. The mechanisms by which IL-1β contributes to neuronal damage remain to be elucidated, but the damage caused by the cytokine seem to be related to its pro-inflammatory properties or to possible changes in glutamatergic calcium influx (Allan et al., 2005).

However, there is evidence that IL-1 can also be neuroprotective. For example intravitreous injection of 4ng IL-1β protects retinal ganglion cells from death after optic nerve axotomy (Diem et al., 2003). This neuroprotective effect of IL-1 is exerted via the phosphinositol-3-kinase/Akt pathway. In the same work it was shown *in vitro* that IL-1β induces an IL-1RI-independent change of sodium and potassium currents via neuronal cell membrane. This decrease of ion-fluxes was counteracted by a specific antibody to IL-1 but not by IL-1ra (Diem et al., 2003). I*n vitro* incubation of primary rat astrocytes with IL-1β leads to high mobility group box 1 (HMGB1) release, a nuclear protein known to contribute to recovery from neuronal stroke (Hayakawa et al., 2010). In a mouse model of Alzheimer's disease, it has been shown that transgenic sustained IL-1β production mitigated amyloid pathology and plaque size (Matousek et al., 2012). Neuronal long time survival was reduced after injection of kainic acid (KA), which induces excitotoxicity by activating glutamatergic AMPA-receptors, into IL-1R-RacPb deficient mice (Gosselin et al., 2013). Thus, whether IL-1 exerts neuroprotective or neurotoxic effects depends on the specific pathologic or physiologic circumstances, on the time point of action and on its concentration.

Another brain function that is influenced by IL-1β is hippocampus-dependent memory. Gibertini et al. showed that infection and intraperitoneal (i.p.)-injection of IL-1β in pyrogenic concentrations lead to an impairment of spatial memory in the Morris water maze test (Gibertini et al., 1995). Other experiments confirmed these findings with different memory paradigms (for review see Pugh et al., 2001). These experiments, however, focussed on exogenous application of IL-1 in concentrations comparable to those under inflammatory conditions, and therefore cannot be used to explain the influence of IL-1β on learning under physiological,

healthy conditions. LTP, considered as model of the cellular mechanisms underlying hippocampal learning, induces IL-1β gene expression in the hippocampus *in vitro* and *in vivo* (Schneider et al., 1998). Moreover, inhibition of IL-1β by IL-1ra leads to a reversible inhibition of LTP maintenance in the hippocampus (Schneider et al., 1998), showing that IL-1β plays a critical role in LTP. Further evidence of the influence of IL-1β on learning was provided by Avital et al, who showed that IL-1RI knock-out mice display deficits in the Morris water maze test as compared to wild-type mice (Avital et al., 2003). Yirmiya et al. showed that transgenic expression of IL-1ra in rats leads to a poorer performance in the same learning paradigm and a poorer passive avoidance response, whereas i.c.v injection of 10ng IL-1β causes memory improvement in the passive avoidance response (Yirmiya et al., 2002). Del Rey et al. showed that a brain-borne cytokine network is not only activated during LTP maintenance but also during learning a hippocampus-dependent task. The expression of IL-1, IL-18, IL-1ra and IL-6 genes is increased in defined regions of the hippocampus during learning in parallel to decreased IL-1ra expression in the prefrontal cortex. This might play a role in certain pathological states, in which the hippocampus and the prefrontal cortex are involved, such as schizophrenia or Alzheimer's disease (del Rey et al., 2013). Thus, it seems that IL-1β in physiologically healthy conditions is needed for hippocampal LTP and spatial memory, whereas in sickness and infection it leads to hippocampal memory impairment and inhibits LTP (Besedovsky and del Rey, 2011). LTP maintenance is dependent on changes in neuronal gene expression (Lynch, 2004). Thus, it seems more likely that LTP induces IL-1β production, which then influences neuronal gene expression in a para- or autocrine way and thereby helps to maintain LTP.

IL-1β can also alter neurotransmitter concentrations in different parts of the brain (Besedovsky and del Rey, 1996) that correlate temporarily with metabolic and endocrine changes. It could be shown that IL-1β reduces noradrenalin concentrations in the hypothalamus, the brainstem and the spinal chord of rats (Kabiersch et al., 1988). Cerebral noradrenergic neurons are known to play a crucial role in the regulation of glucose metabolism, including glucocorticoid secretion and blood glucose levels (Foscolo et al., 2003; Leibowitz, 1988; Ritter et al., 2006). Furthermore, IL-1β-induced hypoglycemia in mice is paralleled by

increased serotonin concentrations in the hypothalamus without evident changes in insulin plasma levels (Ota et al., 2009).

The results discussed above implicate that peripheral cytokines interact with the brain. The question of how peripherally injected or produced cytokines induce changes at brain level is not yet fully understood. Two main routes of communication have been proposed: a quick neuronal route via afferent nerves of the autonomous nervous system, for example the vagus nerve, and a slower humoral route affecting circumventricular organs, the choroid plexus or leading to a signalling via brain vessel endothelia (Dantzer, 2009). Neurons in the vagal nerve express IL-1RI, and intravenous IL-1β injection results in c-fos expression in neurons in the nodose ganglion, reflecting neuronal activation (Ek et al., 1998). These results were confirmed by experiments showing that subdiaphragmal vagotomy decreases the behavioural effects of peripherally injected IL-1β (Bluthe et al., 1996).

The humoral communication pathway is linked to prostaglandins. Injection of cyclooxygenase-2 (COX-2) inhibitors leads to diminished fever response and HPA activation by IL-1β (Parsadaniantz et al., 2000). COX-2 is necessary for the inflammation-induced synthesis of prostaglandins. This shows that prostaglandins are at least in part responsible for the behavioural and endocrine changes induced by IL-1β injection. Furthermore, brain vessels express IL-1RI and show increased COX-2 expression after IL-1β injection (Cao et al., 1997; Parsadaniantz et al., 2000). Gosselin and Rivest showed that endothelial MyD88 is necessary for IL-1-induced neuronal activation and corticosterone release (Gosselin and Rivest, 2008). However, IL-1β-induced behavioural changes do not depend on prostaglandins alone, but also on effects of cerebral IL-1, since the effects of injected IL-1β could be totally abolished by simultaneous i.c.v. injection of IL-1ra (Plata-Salaman and Ffrench-Mullen, 1992). Furthermore, experiments with radio-labelled IL-1 showed that circulating IL-1 enters the brain via a saturable transport system and elicits direct effects in the CNS (Banks et al., 2002; Banks and Kastin, 1991; Banks et al., 1989). For an extensive review of cytokine-brain interaction see McCusker and Kelley, 2013.

1.2.4 IL-1β and energy metabolism

IL-1β induces a profound and long-lasting hypoglycemia in mice. This effect is insulin-independent and is not due to loss of glucose in the urine or decreased

food intake (del Rey and Besedovsky, 1987; del Rey and Besedovsky, 1992; del Rey et al., 2006). Part of this hypoglycemia can be explained by IL-1β-induced glucose uptake by different peripheral tissues, for example adipocytes, fibroblasts, intestinal macrophages and chondrocytes (Bird et al., 1990; Fischereder et al., 2003; Fukuzumi et al., 1996; Garcia-Welsh et al., 1990; Gould et al., 1995; Shikhman et al., 2004).

Glucose uptake is mediated by increased expression of different glucose transporters (GLUT), depending on the tissue. In ovarian granulosa cells, for example, IL-1β induces an increase of GLUT-1 and GLUT-3 expression (Kol et al., 1997), whereas in chondrocytes it induces GLUT-1 and GLUT-6 expression and incorporation into the cell membrane (Shikhman et al., 2004).

Additionally, IL-1β inhibits gluconeogenesis in the liver by inhibiting the phosphoenolpyruvate-carboxykinase and leads to a reduced glycogen content in the liver (del Rey et al., 1998; Metzger et al., 2004).

Some studies suggest that IL-1β may induce hypoglycemia not only in rodents, but also in humans, since low doses of LPS induce a transient hypoglycemia (Bloesch et al., 1993) and increase glucose utilization (Agwunobi et al., 2000). In a phase I trial IL-1β induced a transient hypoglycemia in patients (Crown et al., 1991).

Besides peripheral mechanisms, there is evidence that central mechanisms also contribute to IL-1β-induced hypoglycemia:

(a) C3H/HeJ mice react to IL-1β injection with hypoglycemia that lasts at least eight hours, whereas counterregulatory hormones such as glucagon and corticosterone return to normal levels after four hours (del Rey and Besedovsky, 1987; Ota et al., 2009);

(b) i.c.v. injection of IL-1ra to C57BL/6J mice simultaneously injected with IL-1β i.p. leads to a less profound hypoglycemia than in animals injected with IL-1β alone (del Rey et al., 1998);

(c) IL-1β-injected mice return to hypoglycemia after a glucose load. This effect is abolished by simultaneous i.c.v. injection of IL-1ra (del Rey et al., 1998; del Rey et al. 2006);

(d) IL-1β leads to a decrease of blood glucose values in insulin resistant db/db deficient mice. These animals return to decreased blood glucose values after a glucose load (del Rey et al., 2006).

So far it is unknown if IL-1β changes glucose uptake and consumption in neurons. However, evidence exists that IL-1 increases glucose metabolism and glucose uptake in astrocytes (Vega et al., 2002). The role of astrocytes in cerebral energy metabolism and in neuronal energy supply is not yet fully understood, but recent evidence indicates that astrocytes might play a central role in cerebral and neuronal energy metabolism (see 1.4). The predominant glucose transporter in neurons is GLUT-3, whereas glial cells, such as astrocytes, mainly express GLUT-1 (Simpson et al., 2008; Vannucci et al., 1997). The expression of both isoforms is increased during phases of increased cerebral glucose utilization (increased synaptic connectivity, brain maturation), whereas it decreases in states of decreased cerebral glucose utilization (e.g. Alzheimer's disease, Simpson et al., 2008; Vannucci et al., 1997). One possibility would be that IL-1 induces changes in the expression and incorporation of GLUTs in the cell membrane of neurons and astrocytes, as it does in other tissues (Metzger et al., 2004; Shikhman et al., 2001), which might help to keep the intracellular glucose concentration at the same level during extracellular hypoglycemia. In contrast to activation of the HPA-axis, the hypoglycaemic effect of IL-1 seems to be independent of prostaglandins, since hypoglycemia is not influenced by COX inhibitors (Besedovsky and del Rey, 1987).

1.3 Corticosterone

Corticosterone is the most important glucocorticoid in mice. Glucocorticoids influence various immunological responses. For example, they diminish endothelial permeability, inhibit cytokine production and decrease lymphocyte clonal expansion (Zen et al., 2011). Glucocorticoid levels increase after endotoxin challenge and act as inhibitors of the systemic or local inflammation (Zen et al., 2011). Increased corticosterone blood levels are also observed during specific immune responses and contribute to regulate the magnitude and specificity of the immune response. (Besedovsky et al., 1975; del Rey et al., 1984) Thus, glucocorticoids play an important role in regulating inflammation and immunity, and in regaining the physiological, healthy state after infection (Besedovsky and del Rey, 2006, for review see Besedovsky and del Rey 1996). It is known since a long time that the increase in glucocorticoid levels during an immune response is mediated by immune-derived products (Besedovsky et al., 1985). IL-1 was the

first purified cytokine shown to stimulate the HPA axis. IL-1 injection leads to an increase in ACTH and corticosterone plasma levels. This increase is dose-dependent at least up to a dose of 1 µg/mouse and peaks two hours after injection (Besedovsky et al., 1986). At least the acute IL-1-induced increase of ACTH and glucocorticoid levels is due to effects at hypothalamic levels, by stimulation of CRF release into the hypothalamic-pituitary portal system (Berkenbosch et al., 1987). IL-1-induced prostaglandin synthesis at central levels might be responsible for the hypothalamic effects (Turnbull and Rivier, 1999).

1.4 Astrocyte-Neuron-Lactate-Shuttle

Following the classical view of neuronal energy metabolism, the main fuel for neurons is supplied by glucose, which is oxidized via glycolysis to pyruvate and then delivered into the tricarboxylic acid (TCA) cycle. The reducing equivalents are then reoxidized by the electron transport chain, the major ATP-producing mechanism under aerobic circumstances.

In 1994, Pellerin and Magistretti introduced a new concept of cerebral energy metabolism, named the astrocyte-neuron-lactate-shuttle hypothesis (ANLSH, (Pellerin and Magistretti, 1994). It was shown that glutamate uptake into astrocytes increases glycolysis and lactate release. These results support the hypothesis that astrocytes are the main metabolizers of cerebral glucose and release lactate, which is then taken up by neurons and further metabolized (Pellerin and Magistretti, 1994). It has been shown in different *in vitro* and *in vivo* studies that astrocytes are better suited for glycolysis and lactate production than neurons, whereas neurons are more likely to metabolize lactate than astrocytes (Pellerin, 2008). Lovatt et al. showed in a transcriptome study that glycolytic enzymes are expressed abundantly in astrocytes as compared to neurons (Lovatt et al., 2007). Furthermore, they showed that the expression of lactate-dehydrogenase b (LDHb) is increased more than 13-fold in astrocytes relative to neurons, whereas expression of LDHa is increased 8-fold in neurons relative to astrocytes. In principle, LDHb catalyses the hydrogenation of pyruvate to lactate, whereas LDHa catalyses the reverse reaction. Thus, astrocytes are better suited to produce lactate from pyruvate, whereas neurons are more suited to produce pyruvate from lactate, providing arguments in favour of the ANLSH. In the same study, using radio-labelled glucose, it was shown that astrocytes produce lactate

directly from glycolysis. Surprisingly, some of the lactate originated from TCA-cycle intermediates, suggesting that not all glucose was metabolized to lactate, but some was transferred to the TCA cycle (Lovatt et al., 2007).

It is still controversial if and how energy metabolism is compartmentalized in the brain between astrocytes and neurons. It is still unclear whether glucose is primarily taken up by neurons or astrocytes, if lactate is shuttled between these cells and if lactate contributes to brain energy metabolism in a significant amount at all (Chih et al., 2001; Mangia et al., 2011; Pellerin, 2008).

1.5 Central glucose-regulation

A necessary condition for central glucose regulation is the presence of cells able to sense glucose or its metabolites to assess the state of energy metabolism in the brain and in the whole body. These glucose-sensing neurons are found in different parts of the brain such as the brain stem and different nuclei of the hypothalamus as first shown by Oomura in 1969 (Oomura et al., 1969). Glucose-sensing neurons can be divided into glucose-excited (GE) neurons, which depolarise when glucose concentration rises and hyperpolarise when glucose concentration decreases, and glucose-inhibited (GI) neurons, which hyperpolarise when glucose concentration rises and depolarise when glucose concentration decreases (Burdakov et al., 2005).

Glucose-sensing neurons can be classified based on the neurotransmitter they release or on their location:

(a) Glucose-sensing neurons, which release products of the pro-opiomelanocortin (POMC) gene or neuropeptide Y (NPY) upon depolarisation are found in the arcuate nucleus of the hypothalamus. These neurons play a crucial role in food intake and catabolic or anabolic energy metabolism and do not only react to changes in glucose concentrations but also to leptin or insulin, hormones that indicate the state of feeding and energy storage (Cone et al., 2001).

(b) Orexin-producing glucose-sensing neurons in the lateral hypothalamus play a role in feeding behaviour (possibly mediated via the NPY/POMC system) and the regulation of sleep and wakefulness (Sakurai, 2007).

(c) Concerning counterregulation to hypoglycemia, glucose-sensing neurons in the ventromedial hypothalamus (VMH) are of great importance. Lesions in

the VMH cause a significant decrease in counterregulatory hormones during hypoglycemia compared to lesions in the lateral hypothalamus or sham-operated animals (Borg et al., 1994). Moreover, local infusion of D-glucose into the VMH results in a decreased release of counterregulatory hormones during a hypoglycaemic clamp (Borg et al., 1997), whereas infusion of 2-deoxyglucose into the VMH induces an increase in hypoglycaemic counterregulatory hormones. 2-deoxyglucose enters cells as glucose but is not further metabolized and therefore causes intracellular hypoglycemia (Borg et al., 1995).

GE- and GI-neurons can be identified in the VMH. The depolarisation of GE-neurons is mediated by an ATP-sensitive K^+-channel (K_{ATP}-channel). K_{ATP}-channels close at high concentrations of ATP which leads to depolarisation of the respective cell (Ashford et al., 1990). Infusion of diazoxide, a potassium channel opener, into the VMH augments counterregulatory responses to hypoglycemia, whereas infusion with sulfonylurea inhibits counterregulatory responses by closing K_{ATP} –channels (Evans et al., 2004; McCrimmon et al., 2005; Sherwin, 2008). These findings indicate that excitation of GE-neurons leads to decreased hypoglycaemic counterregulation, whereas hyperpolarisation of GE-neurons in the VMH induces hypoglycaemic counterregulation. Furthermore, it could be hypothesised that glucose metabolites might be able to influence glucose-sensing neurons as well. In fact, lactate stimulates GE-neurons *in vitro* (Song and Routh, 2005) and lactate infusion into the VMH leads to a decrease of epinephrine, norepinephrine and glucagon plasma concentrations in hypoglycaemic rats and an 8-fold increase in glucose infusion rate needed to maintain hypoglycemia in an euglycaemic/hypoglycaemic clamp (Borg et al., 2003).

1.6 Magnetic resonance spectroscopy

1.6.1 Operation principle

The basic principle of magnetic resonance spectroscopy (MRS) as used in this study is the proton (H^1) magnetic resonance imaging technique.

In H^1 magnetic resonance imaging (MRI), the spin of hydrogen nuclei consisting of a single proton is used to induce alterations in an external magnetic field. The spin of atomic nuclei is an innate property of the respective atom. The spin itself is not

detectable, but since the nucleus has a positive charge, the spinning produces a magnetic momentum and acts like a dipole.

MRI devices work with different magnetic fields and electromagnetic impulses. The strong external magnetic field B_0 induces a precession of the spin. The frequency of the spin precession is called Larmor-frequency. The Larmor-frequency is specific for each nuclear isotope and proportional to the strength of the external magnetic field. The strong magnetic field effectuates a longitudinal magnetisation, which can be detected and switched in a 90° angle with a radiofrequency impulse of the Larmor-frequency called resonance impulse. Now nuclear spins do not precess longitudinally but transversally, which induces an alternating current of the Larmor-frequency in a reception coil. This is the MR-signal (Weishaupt et al., 2009).

Whereas standard MRI is used to obtain spatial information, MRS is used to obtain information about the chemical composition of the examined subject *in vivo*. H^1 nuclei in different chemical compounds are surrounded by different electron clouds. These electrons lead to a slight change in the strength of the magnetic field that acts on the nucleus. Since the Larmor-frequency is dependent on the strength of the magnetic field, the result is a slight shift of this frequency. This shift is measured and, after different calculations, plotted on a graph with the chemical shift in parts per million (ppm) on the X-axis. The vertical Y-axis plots the relative signal amplitude. Thus, the concentration of the determined metabolites is proportional to the area under the curve of the respective peak (Backens, 2010).

1.6.2 Metabolites

N-acetyl aspartate

N-acetyl aspartate (NAA) is present at high concentrations in the brain and gives the largest peak in healthy brain MRS, resonating at 2.02 ppm (Soares and Law, 2009). It is used as a marker of neuronal integrity since its concentration decreases in various states of neuronal loss such as stroke, neurodegenerative diseases, multiple sclerosis (MS) or gliomas (Barker and Lin, 2006). Furthermore, it has been shown that lower concentrations of NAA correlate with higher disability scores in MS, indicating its usefulness as marker of neuronal function (de Stefano et al., 2001). However, patients with Canavan's disease, a fatal, genetic disorder of NAA catabolism, show a marked increase in NAA concentration but a severe impairment of motor and cognitive development. Canavan's disease is the only

disorder known so far that involves increased NAA concentrations, thus showing restrictions to the usefulness of NAA as marker for neuronal integrity (Moffett et al., 2007).

Despite its high concentration in the brain, its function remains controversial. There are four major theories concerning the role of NAA in brain:

a) NAA is synthesized in neurons and shuttled to oligodendrocytes, in which the acetyl moiety is cleaved from aspartate and used for lipid synthesis, thus serving for myelination; b) NAA is considered as an organic osmolyte, equalling the anion deficit in neurons or being used for co-transport with intracellularly synthesized water; c) NAA is a precursor of the dipeptide *N*-acetyl aspartyl glutamate (NAAG), a neuropeptide that influences presynaptic excitability; d) NAA is linked to oxidative energy metabolism. However, it is still unclear whether it plays a role in energy metabolism (Moffett et al., 2007).

Lactate

Lactate is the product of the lactate-dehydrogenase (LDH) reaction, when pyruvate is reduced to lactate while NADH is oxidized to NAD^+. This reaction mainly occurs under anaerobic conditions. Its main function is to restore NAD^+, which is necessary for glycolysis. In some tissues, such as the liver, the LDH-reaction is reversed and lactate is used for glycogenesis or enters the tricarboxylic acid (TCA) cycle via oxidation to pyruvate.

In MRS, the methyl group of lactate resonates at 1.31 ppm. Rises of lactate concentration under hypoxic conditions or states of increased anaerobic glycolysis, such as seizures, can be detected with cerebral MRS (Soares and Law, 2009). Some studies show an increase in lactate in the visual cortex under physiological photic stimuli (Prichard et al., 1991; Sappey-Marinier et al., 1992), whereas others could not reproduce these results (Merboldt et al., 1992).

Creatine

Creatine (Cr) is synthesized in the liver and kidney, and transported via blood to other tissues, where it is taken up by active transport. It acts as “energy-buffer” since it can be phosphorylated to phosphocreatine by the enzyme creatine kinase. The phosphate group of creatine phosphate (PCr) can be used to phosphorylate ADP to ATP, which is important in tissues with a high energy metabolism, such as muscle, spermatozoa or brain (Wallimann et al., 1992).

The methyl group of Cr and PCr resonates at 3.03 ppm. Thus Cr and PCr are not distinguishable by H^1-MRS (Soares and Law, 2009). Although Cr concentration is considered to be temporally stable its concentration varies between different brain regions. Albeit its common use to calculate metabolite ratios (Barker and Lin, 2006), it was not used as reference in the studies reported here since Cr is also involved in energy metabolism.

Choline

The $C(NH_3)_3$ group of Cho resonates at 3.20 ppm. The resulting peak is composed of soluble glycerophosphocholine, phosphocholine and free choline. The choline bound to macromolecules of the membranes is not detected by MRS. Choline levels differ between white and grey matter and change during pathological states. Higher choline levels might be found in tumor tissue, whereas its levels usually decrease in situations such as infections or degeneration (Soares and Law, 2009).

1.7 Aims and objectives

This work consists of two parts. The first part investigates the question if IL-1β-induced hypoglycemia is MyD88-dependent. To answer that question, MyD88KO mice were injected with IL-1β and blood glucose and corticosterone levels were compared to their WT littermates, which received the same treatment. MyD88KO mice show no obvious abnormalities in their development as compared to WT mice. However, if alternative signalling mechanisms, especially in the brain, are developed due to the lack of MyD88 is not known. Therefore, a pharmacological MyD88 inhibitor was used as a second approach to answer that question. WT mice received either the inhibitor or a control peptide prior to IL-1β injection and blood glucose and corticosterone levels were measured and compared.

The second part of this work focuses on cerebral energy metabolism under IL-1β induced hypoglycemia. As discussed above, IL-1β resets glucose homeostasis at central levels. Thus, cerebral energy metabolism must be influenced. To describe this and compare it to cerebral energy metabolism under insulin-induced hypoglycemia, WT mice were injected with IL-1β, insulin or vehicle and cerebral H^1MRS was performed. Thus, it was possible to compare the metabolite-changes *in vivo* and during the course of hours, since MRS can be repeated several times in the same animal. Three of the four metabolites detected are involved, or

supposed to be involved, in energy metabolism. As opposed to Lac and NAA, the mechanisms by which Cr contributes to energy metabolism are well understood. According to the controversially discussed ANLS Hypothesis, astrocyte-derived lactate is shuttled to neurons to meet with the neuronal energy demand. NAA might be linked to oxidative energy demand. Cho, the fourth metabolite detected, is not involved in energy metabolism and used as reference substance in this work.

2 MATERIAL AND METHODS

2.1 Animals

C57BL/6J male mice (7 week-old) were purchased from Harlan Winkelmann (Borchen, Germany). MyD88 KO mice were used after obtaining written permission from Dr. S. Akira, University of Osaka, Japan. The MyD88 KO mice for evaluating the MyD88-dependence of IL-1β-induced hypoglycemia were kindly provided by Prof. Dr. Dalpke and Dr. Bode, Institut für medizinische Mikrobiologie und Hygiene, Heidelberg. These MyD88KO mice have a C57BL6/J background.
MyD88-deficient mice are fertile and breed normally. In general, breeding was started with one female and one male. Pups were fed by the mother until they were three to four weeks old. The offspring was identified by ear-marks and the tip of the tail was collected for genotyping. Thereafter, pups were separated from the mother, according to the gender, and kept in groups of not more than 4 animals per cage.
All animals were housed permanently in a humidity-, temperature- and light- (12h cycle) controlled room. Animals were fed with normal chow diet and had access to food and water *ad libitum.* Animals were individually caged for at least 7 days before experiments were started. To control the health status and to accustom the animals to handling, mice were weighted twice a week. Only male mice between 8 and 17 weeks of age (b.w. 20-30 g) were used for the experiments. The distribution in the different experimental groups was weight- and age-matched. Experiments were approved by the Regierungspräsidium Gießen (Aktenzeichen V54-19c 20-15(1) MR 20/28-Nr. 59/2007).

2.2 Material

The instruments, materials and software used in this work are listed in the tables below.

Table 1: Instruments

Instrument	Product name	Producer
Autoclave	Omega media	Prestige medical, USA
Balance	METTLER PM 3000	Mettler Toledo GmbH, Germany

Blood glucose meter	Accu Chek Sensor	Roche Diagnostics; Germany
Centrifuge 1	Table centrifuge Heraeus Pico 17	Heraeus Holding GmbH, Germany
Centrifuge 2	Biofuge Fresco	Heraeus Holding GmbH, Germany
Gradient system	BGA 20S (gradient strength: 290 mT/m, slew rate: 1160 T/m/s)	Bruker BioSpin, Germany
Lactate meter	Cobas	Accutrend Plus
Microplate reader	Tecan Sunrise	Tecan group Ltd., Switzerland
MRI/MRS scanner	Remote ClinScan, 7 Tesla MRI/MRS scanner	Bruker Daltonics, Germany
Pipettes	Pipette 0,5 - 10 µl, 200 - 1000 µl	Eppendorf AG, Germany
Pipettes	Pipetman 0 -20 µl, 0-200µL	Gilson, France
Ear punch plier	Nadox KN292B stainless 2.0	
Respiratory frequency monitor	Monitor respiratory frequency	SA Instruments, Australia
Spectrophotometer	Ultrospec 2000	Amersham Pharmacia Biotech GmbH,Germany
Surface head coil	2-channel quadrature surface head MRI coil	Rapid biomedicals, Bruker
Surgical blade	Sterical carbon steal blade	Heinz Herenz, Germany
Water bath system	Haake P5 + C10	Thermo Electron Cooperation

Table 2 Materials

Material	**Product name**	**Producer**

Breeding diet for mice	LASQCdiet Rod16, Hihyg (pasteurised)	Lasvendi, Germany
Canula	Single-use-injection canula Sterican	B. Braun Melsungen AG, Germany
Capillaries (75 µl)	Haematocrit-Capillaries Sodium-heparinized 3,75 U/capillary	Hirschmann Laborgeräte, Germany
Gloves	Nobaglove-Latex	Noba Verbandmittel Danz GmbH u. Co KG, Germany
Microtube	Microtube 0,5 ml	Sarstedt, Germany
Normal diet for mice	Lasqcdiet Rod18, Hihyg (pasteurised)	Lasvendi, Germany
Pipette tips	Pipette tips, 10 µl, 20 µL, 200 µL, 1000µL	Gilson, France
PCR cycler 1	Hybaid Cycler	Omni Gene Bioproducts, USA
PCR cycler 2	Sensoquest labcycler	Sensoquest, Germany
Single-use-Syringe	1 ml Norm-ject	Henke-Sass, Wolf, Germany
Test stripes blood glucose	Glucose test stripes Accu Chek Sensor Comfort Test	Roche Diagnostics, Germany
Test stripes blood lactate	stripes for lactate Cobas Accutrend Plus	Roche, Germany
Tube 1,5 ml	Micro tube 1,5 ml	Sarstedt, Germany
Tube 2,0 ml	Micro tube 1,5 ml	Sarstedt, Germany

Table 3 Reagents

Reagent	**Product name**	**Producer**
Agarose	Agarose ultra PURE	Gibco Invitrogen, Germany

AmpliTaqGold	AmpliTaqGold	Applied Biosystems, Germany
Base ladder	GeneRuler. 100 bp DNA Ladder	Fermentas, Thermo Scientific, Germany
Bepanthen	Bepanthen, Eye and Ear cream	Bayer healthcare, Germany
Diethylether	Diethyl ether puriss. stabilized	Sigma-aldrich, Germany
DNA purification	QIAquick Gel extraction Kit	Qiagen, Germany
dNTP(10 mM)	RT Kit Cat No 18064-0220	Invitrogen, Germany
DTT (0,1 M)	RT Kit Cat No 18064-0220	Invitrogen, Germany
Ethanol	Ethanol 99,8%	Carl Roth, Germany
Ethanol	Ethanol 75%	Riedel de Haen, Germany
GelRed	GelRed Nucleic Acid Gel Stain	Biotium, USA
H2O	H2O ultra pure water	Nanopure ultra pure water system, Marburg, Germany
HCl	Hydrochloric acid	Merck, Germany
IL-1β	Human recombinant IL-1β	Glaxo Institute for Molecular Biology, Switzerland
MyD88 inhibitory peptide	IMG2005	Imgenex, USA
Control peptide	Control peptide	Imgenex, USA
Insulin	Insulindetemir (Levemir ®), 100 E (14,2 mg) per 1 ml	Novo Nordisk, Dänemark
Isoflurane	Isoflurane HDG9623	Baxter GmbH, Germany
KCl	Potassium Chloride	Merck, Germany

MgCl2	Magnesium Chloride	Merck, Germany
NaCl	Sodium Chloride	Merck, Germany
NaCl (0,9%)	Sodium chloride solution, isotone	B. Braun Melsungen AG, Germany
Corticosterone ELISA kit	Corticosterone ELISA	IBL International GmbH, Germany
Oligo dT primer	Oligo $d(T)_{12-18}$	Amersham Pharmacia Biotech GmbH, Germany
Primer	See Table 2	Tib MolBiol, Germany
Proteinase K	Proteinase K	Qiagen, Germany
Reverse transcription buffer (5x)	RT Kit Cat No 18064-0220	Invitrogen, Germany
RNase free DNase I	RNase free DNase I (1U/µl)	Epicentre, USA
RNase free H2O	RNase free H2O	Qiagen, Germany
Rox reference dye	Rox reference dye	Agilent Technologies, Germany
SDS	Sodium Dodecyl Sulfate	Fluka BioChemika, now Sigma Aldrich, Germany
Solution for Rnase decontamination	Qiagen RNeasy Kit Rnase-away	Invitrogen, Germany
SuperScriptII (200 U/µl)	RT Kit Cat No 18064-0220	Invitrogen, Germany
TAE buffer	Tris-Acetat-EDTA buffer	Fermentas, Thermo Scientific, Germany
Tango buffer (10x)	10x Y+/Tango Tango buffer	MBI Fermentas, Thermo Scientific, Germany
TRIS	TRIS Reagent	Carl Roth, Germany
Trizol	Trizol	Invitrogen, Germany
Tween20	Polyethylene glycol sorbitan monolaurate Polyoxyethylene - sorbitan monolaurate Polysorbate	Sigma-Aldrich, Germany

	20	
Uracil-DNA-glycosylase	Uracil- DNA- glycosylase	New England BioLabs, Germany

Table 4 Software

Software	Product name	Producer
ELISA	Evaluation MagellanTM	Tecan Group Ltd., Switzerland
Statistical Software	IBM SPSS Statistics 20	IBM
Writing Software	Microsoft Office Word 2003	Microsoft

2.3 Methods

2.3.1 Gentoyping

The genotyping was kindly carried out by Dr. A. Randolf. using polymerase chain reaction (PCR). PCR was conducted with the primers shown in Table 5 adapted from Leadbetter et al 2002 (Leadbetter et al., 2002). DNA was obtained from the tip of the tail. A negative control and three genotype controls (heterozygous, MyD88KO and MyD88 wild-type) were included in each typification round. The PCR was conducted in a total volume of 25 µL containing: 1µl template, 12.5 µL 2x Taq PCR master mix kit, Quiagen, 0.2 µL of each primer (10mM) and 8.5 µL H_2O. Sequences of the primers are shown in table 5. The cycler program was started with 2 minutes at 95℃ followed by 30 ampli fication cycles of 95℃ for 30 sec, 60℃ for 45 sec, 72℃ for 45 s and finished wi th 72 ℃ for 5 min, using Sensoquest labcycler. PCR products were separated by agar gel electrophoresis. Samples from heterozygous mice showed two bands, one at 550 base pairs (bp) and one at 600 bp, samples from WT mice showed one band at 550 bp and samples from MyD88KO animals showed one band at 600 bp.

Table 5: Primers used for PCR.

Primer	Sequence
MyD88 forward	5' - TGG CAT GCC TCC ATC ATA GTT AAC C - 3'
MyD88 reverse	5' - GTC AGA AAC AAC CAC CAC CAT GC - 3'
MyD88 neo	5' - ATC GCC TTC TAT CGC CTT CTT GAC GAG - 3'

2.3.2 Injection

All injections were performed i.p. Since injections were always carried out immediately after the first blood collection to determine basal values, mice were still under narcosis when injected.

2.3.3 Blood collection

Blood was obtained from the tip of the tail under light diethylether narcosis, with exception of the MRS experiments. For narcosis, animals were initially placed in a glass box containing a diethylether soaked towel. When the tail pinch reflex was abolished, the procedure was started. To maintain narcosis during the procedure, the neck of the mice was placed in a glass flask containing ether-soaked paper towels. Whole blood was used for glucose determination. An additional blood sample was collected in heparized hematrocrit tubes and immediately centrifuged at 16060 g for 10 minutes at 4℃. The plasma was aliquoted and stored at -20℃ until further use for corticosterone determination. After blood collection, the tip of the tail was cauterized.

2.3.4 Glucose determination

Glucose determinations were performed using the AccuCheck Sensor® from Roche Diagnostics. For this purpose, a drop of blood (aproximately 4 µl) is directly placed onto the test stripe, in which glucose is oxidized to gluconolacton by the enzyme glucose dehydrogenase while hexacyanoferrate (III) is reduced to hexacyanoferrate (II). An electrode consisting of palladium re-oxides the hexacyanoferrate (II). The resulting electron flow correlates with the glucose concentration in the blood sample. The measurable concentration ranges from 10 to 600 mg/dl.

2.3.5 Corticosterone determination

Corticosterone concentrations were determined in plasma using a commercially available ELISA kit (IBL international, Germany). The microtiter wells of this ELISA kit are coated with a polyclonal antibody against corticosterone. The corticosterone in the sample competes with horseradish-peroxidase-conjugated corticosterone. The higher the corticosterone concentration in the sample, the lesser horseradish-peroxidase-conjugated corticosterone remains bound to the wells after washing. After addition of the substrate Tetramethylbenzidine, the

intensity of the colour developed is inversely proportional to the amount of corticosterone in the tested sample. The standards provided with this kit range from 0.17 µg/dl to 8.32 µg/dl. To remain within the range of the standards, samples had to be diluted. Samples of IL-1β-injected wild-type animals and all determinations after MRS scan were diluted 1:10, all other samples were diluted 1:3. These dilutions allowed detection of corticosterone concentrations ranging from 0.51 µg/dl to 24.96 µg/dl in 1:3 diluted samples and from 1.7µg/dl to 83.2µg/dl in 1:10 diluted samples.

2.3.6 Magnetic resonance spectroscopy

Magnetic resonance spectroscopy (MRS) was performed in the Centre for Small Animal Imaging, Marburg, Germany. A 7 Tesla (T) MRI/MRS scanner (ClinScan, BRUKER, Bremen, Germany) using syngo MR B15 software (Siemens, Erlangen, Germany) with the gradient system BGA 20S (gradient strength 290 mT/m, slew rate 1160 T/m/s) was used to acquire MR spectral data. A 2-channel quadrature surface head MRI coil was used to receive the signal. Narcosis was initiated by placing mice into a gas chamber which was linked to an isoflurane vaporizer. For initiation, a mixture of 5% isoflurane and 95% room air was lead into the chamber. When tail pinch reflex was absent, narcosis was maintained with 1.5%-3.5% isoflurane and blood collection started. Narcosis was maintained during the MRS procedure using the same vaporizer. To monitor depth of narcosis, breath rate was monitored permanently and kept between 40 and 80 breaths per minute. After narcosis and blood collection, animals were placed on the MRI bed slider and fixed by the front teeth. This allowed administering isoflurane directly to the nose of the animals. Furthermore, animals were fixed carefully by the ears to minimize inaccuracy in positioning. To avoid eye drying, Bepanthen ointment (Bepanthen Eye and Nose ointment, Bayer, Germany) was applied onto the eyes. Hypothermia was prevented by a water-bath system adjusted to 42℃ in the bed slider. Respiratory frequency was monitored by a system (SA Instruments, Burwood East, Australia) with a sensor placed under the chest of the animals.

The MRS protocol starts with a localizer sequence with a repetition time (TR) of 23 ms and an echo time (TE) of 4 ms, slice thickness 1 mm, field of view (FoV) 55 mm and a matrix of 256 pixels to control positioning of the animal. For determination of the Volume of Interest (VOI), three T2 weighted sequences (Turbo Spin Echo, TR 2750 ms (sagital and coronar), TR 3234 ms (transversal);

TE 43 ms; slice thickness 0.7 mm; FoV 28 mm; FoV phase 89.6%; matrix 192; number of slices: sagital 17, coronar 11, transversal 20) were measured. The VOI (which included the third ventricle, hippocampus and striatum excluding the fourth ventricle and the cortex) extends 5.5 mm from bregma 1.3 mm to – 4.2 mm, 6.0 mm right to left, 3.0 mm anterior to posterior (Figure 2).

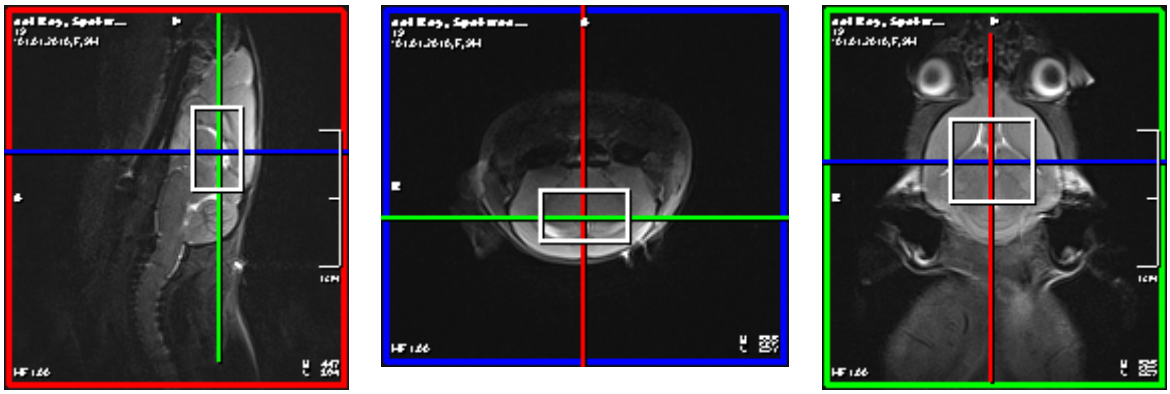

Figure 2 Placement of the VOI in sagittal, coronal and transversal plane (from left to right).

Before spectroscopy was started, the stimulation frequency, signal amplitude and magnetic field were adjusted to keep deviation of frequency below 0.2 ppm. Spectroscopy was performed with a relaxation time of 3000 ms, an echo time of 27 ms and 256 averages at full width half maximum of 46-89 Hz. The water signal was saturated at 200 Hz, and the spectral water suppression (2.35 ppm) was turned on. All spectroscopy data were post-processed with the MR scanner syngo MR software (Siemens, Erlangen, Germany). Post-processing included Gauß filter, Fourier transformation, baseline, frequency and phase corrections and Gaussian line shape fit. The following substances were identified: NAA at 2.02 ppm, Cr at 3.02 ppm, Cho at 3.22 ppm and Lac at 1.33 ppm. The overall duration of the procedure was 35 minutes on average per scan. After MRS data acquisition, blood was collected and animals were placed in their individual cages until next scan.

2.4 Substances and Vehicles

IL-1β: Purified human recombinant IL-1β was kindly provided by A. Shaw (Glaxo Institute for Molecular Biology, Geneva, Switzerland) and diluted to the desired concentration with endotoxin free 0.9% NaCl containing 0.01% human serum

albumin (HSA). The IL-1β doses used in this work are sub-pyrogenic and do not affect food intake.

Insulin: Insulin (long lasting Insulin, Levemir®, Novo Nordisk) 100 Units per ml (U/ml) was diluted to a concentration of 0.5 U/ml with 0.9% NaCl and administered i.p. at a dose of 4 U/kg bodyweight (b.w.).

IMG2005: This is a synthetic polypeptide that inhibits MyD88 homodimerization. IMG2005 and its control peptide were purchased from Imgenex (San Diego, USA). The inhibiting peptide contains two domains. The protein transduction domain (PTD) allows the peptide to enter into the cell, whereas the inhibiting domain binds to the TIR-domain of MyD88 and inhibits its homodimerization which is necessary to recruit downstream kinases in the signalling cascade (Loiarro et al., 2005). The control peptide consists only of the PTD, therefore its molecular weight is lower (2361 Da) than that of IMG2005 (3100 Da). The inhibitor and its control peptide were dissolved and diluted in phosphate buffered saline (PBS).

Vehicle: If not further specified 0.9% NaCl containing 0.01% HSA was used as vehicle.

2.5 Experimental setups

All experiments were started between 8:00 and 10:00 a.m. to avoid influences of circadian rhythm on blood glucose and corticosterone levels. Mice were weighted immediately before initiating narcosis. The results of glucose and corticosterone concentrations corresponding to the first blood sample were defined as base levels (time 0) in all experiments. Blood collection and glucose and corticosterone determinations were performed as described in sections 2.3.3, 2.3.4, and 2.3.5, respectively.

2.5.1 Effect of IL-1β injection on blood glucose and stimulation of the HPA-axis

After obtaining the first blood sample, either 0.2 µg IL-1β in 200 µl vehicle, insulin or 200 µl vehicle alone were injected i.p. Insulin (4 U/kg b.w.) was injected at a concentration of 0.5 U/ml, so the injected volume ranged from 160 to 280 µl, depending on the bodyweight. Six groups were included in this experiment: MyD88-deficient mice that received either IL-1, insulin or vehicle, and the corresponding wild-type C57 BL6/J mice. Substances were injected i.p.

immediately after collecting basal blood sample. Additional samples were obtained 2, 4, 6, 8 and 24 hours after injection (Figure 3).

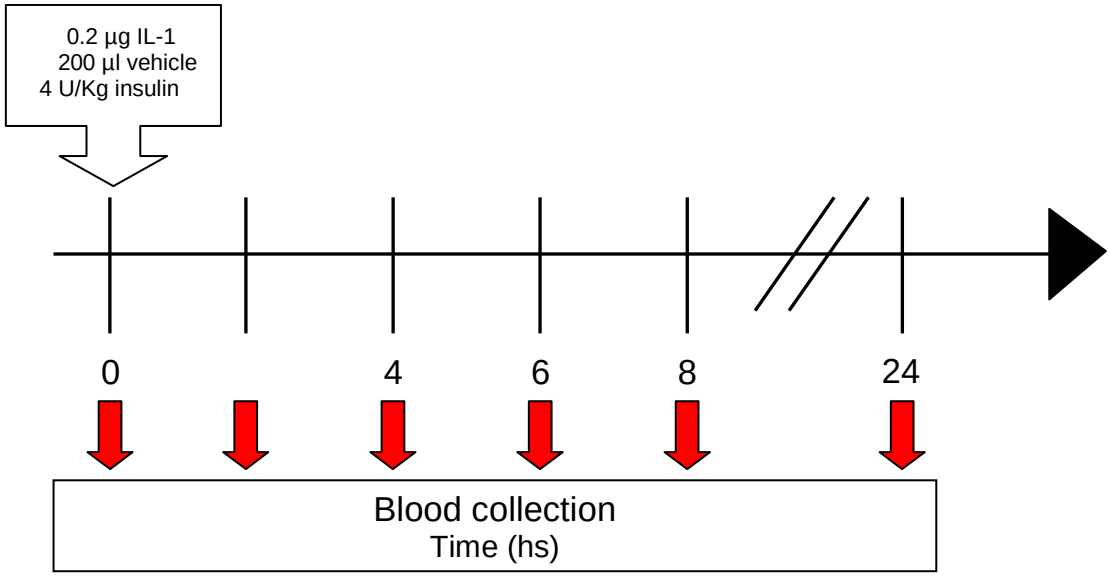

Figure 3 Experimental design to study the effect of IL-1β in MyD88 KO mice.

Blood was taken at time 0 and either IL-1β (0.2 µg in 200µL vehicle), insulin (4 U/KG b.w.), or vehicle (200µL) was injected i.p. Additional blood samples were obtained at the time points indicated.

2.5.2 Pharmacological inhibition of MyD88 signalling

Immediately after obtaining a first blood sample (time 0), mice received 25µg of either IMG2005 or control peptide dissolved in 200µl PBS injected i.p. One hour later, a second blood sample was collected, and immediately after animals received either 0.1µg IL-1β dissolved in 200µl vehicle or 200µl of the vehicle alone. Thus, 4 groups were included in this study. Four additional blood samples were obtained every two hours afterwards (Figure 4).

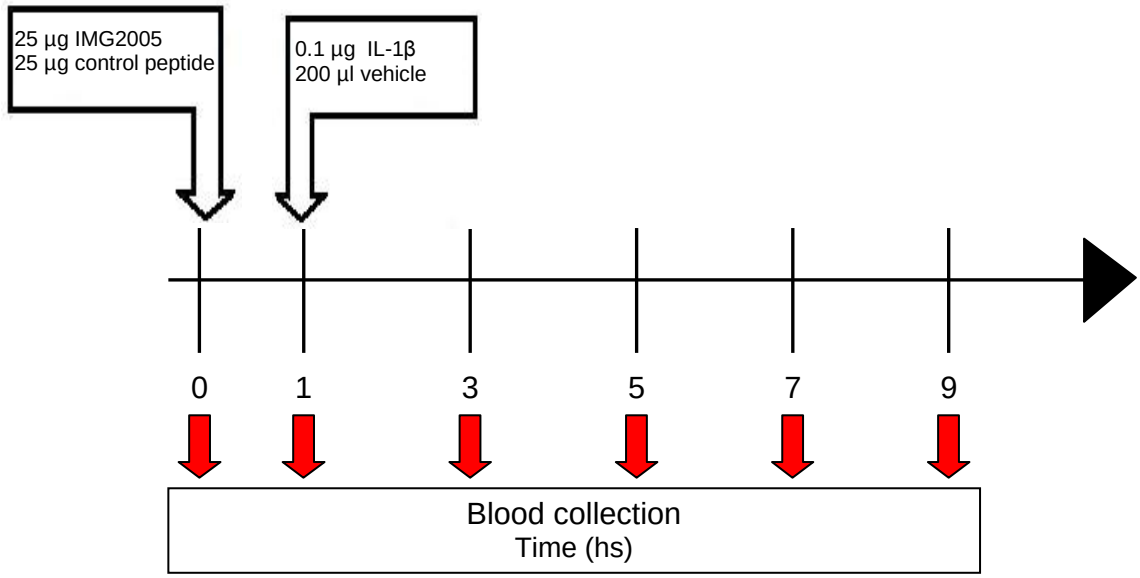

Figure 4 Experimental design to study the effect of inhibiting MyD88 signalling *in vivo.*
Blood was taken at time 0 and animals received either IMG2005 or the control peptide injected i.p. One hour later, blood was collected again and animals received either IL-1β or vehicle injected i.p. Additional blood samples were collected at the time points indicated.

2.5.3 Magnetic resonance spectra of IL-1β-, insulin- and vehicle-injected mice

One week prior to the experiments, animals were brought to the facilities of the Centre for Small Animal Imaging, Marburg for acclimatisation and caged individually. After the first blood collection and glucose determination, MRS data were acquired as described in 2.3.6. The spectrum was defined as time 0 and represents the basal values of the substances evaluated. Immediately after obtaining the first spectrum, a second blood sample was obtained and animals received either 0.1 µg IL1-β in 200 µl vehicle, insulin or 200 µl vehicle injected i.p. An insulin dose of 4 U/kg b.w. was injected i.p. at a concentration of 0.5 U/ml, so that the injected volume ranged from 200 to 240 µl, according to bodyweight. Animals were replaced in their cages until the next MRS acquisition was performed. Thus, the experimental design included 3 groups. Spectra were obtained again 2, 4, 6 and 8 hours after the first MRS recording (time 0), and blood was obtained before and after each scan (
Figure 5). To maintain the same hypoglycaemic level as that induced by IL-1β, it was necessary to repeat the injection of the same dose of insulin (4 U/kg b.w.) after 4 hours.

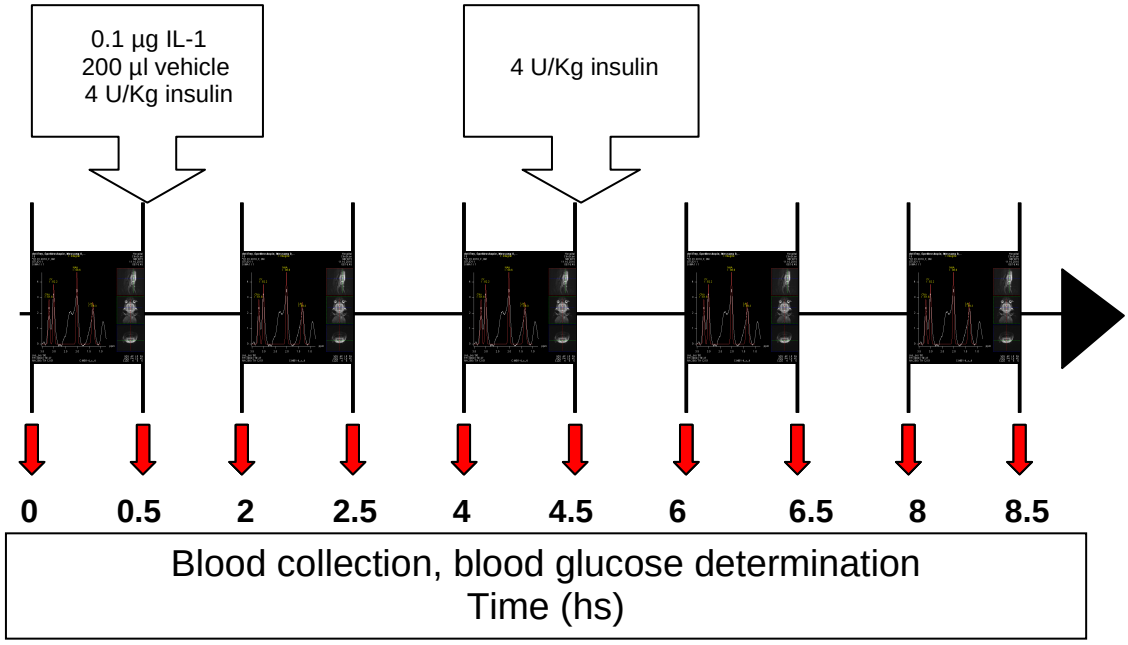

Figure 5 Experimental design of the MRS study. After blood collection and glucose determination the first (basal) MRS was performed. Immediately after, another blood collection and glucose determination were carried out and animals received IL-1β, insulin or vehicle i.p. Further MRS were performed at the times indicated above. Immediately before and after each MRS, blood collection and glucose determination were carried out. Four hours after the first insulin injection, a second insulin injection was necessary to maintain a hypoglycemia comparable to that of the IL-1β injected animals.

2.5.4 Influence of isoflurane on insulin-induced hypoglycemia

Before the first blood collection, mice were narcotized with isoflurane as described above for the MRS determinations. Narcosis was maintained for 35 minutes at an isoflurane concentration of 2.0 %, and a second blood sample was collected. Immediately after, animals received either 200 µl vehicle or insulin. Insulin (4 U/kg b.w.) was injected at a concentration of 0.5 U/ml, so the volume injected ranged from 200 to 240 µl, depending on the b.w. The same procedure, but without injections, was repeated every two hours (narcosis, blood collection, 35 minutes narcosis, blood collection). Since the effect of insulin vanishes after 4 hours, this group of mice received a second insulin injection after 4 hours (Figure 6).

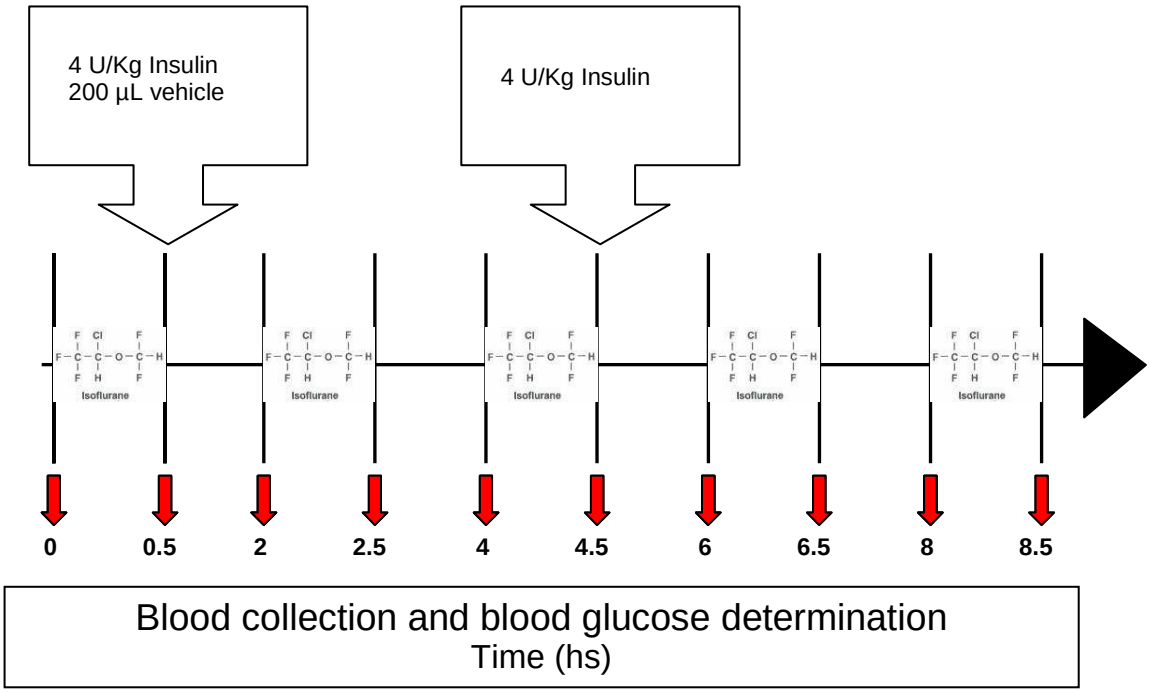

Figure 6 Experimental setup: effect of isoflurane on glucose levels. Blood was collected and blood glucose determined (time 0). After 35 minutes of isoflurane narcosis and another blood collection and glucose determination, the animals received either Insulin or vehicle injected i.p. Further isoflurane narcosis followed at the time points indicated above. Immediately before and after each narcosis, blood was collected and glucose determined. A second insulin injection four hours after the first one was necessary to maintain hypoglycemia at levels comparable to those of the hypoglycemia induced by IL-1β.

2.6 Statistical analyses

The program SPSS version 20 was used for statistical analyses. For experiments in which more than 2 groups were included, one-way analysis of variance (ANOVA) followed by Fisher's least square difference test (LSD) was used to evaluate the results. Student's *t*-test was used to test for statistical difference in experiments consisting of 2 groups. Results were considered statistically significantly different for p-values below 0.05. Unless otherwise specified, results are given as mean ± standard error of the mean (SEM). Outliers were identified by Dixon's Q-test at a 95% confidence level.

3 RESULTS

3.1 IL-1β effects on glucose and corticosterone blood levels are MyD88-dependent

The aim of these experiments was to investigate if the effect of IL-1 on glucose and corticosterone blood levels is dependent on the MyD88-signalling pathway. Although most of the effects exerted by IL-1β are mediated by this pathway, it has been shown relatively recently that an IL-1β MyD88-independent, Akt-kinase signalling mechanism exists in neurons in the anterior hypothalamus (Davis et al., 2006). Furthermore, an IL-1RI-independent effect of IL-1β on ischemic brain damage has been demonstrated (Diem, 2003). Thus, the response of MyD88 KO mice to IL-1β administration on glucose and corticosterone blood levels was compared to that of wild type mice (C57BL/6J). Additionally, the capacity of insulin to induce hypoglycemia in MyD88 KO mice was studied simultaneously in another group of animals.

3.1.1 No effect of IL-1β on blood glucose levels in MyD88 KO mice

The absolute glucose concentrations are shown in figure 7. Since there was a statistically significant difference in basal glucose levels between WT (201±27.62 mg/dl) and MyD88 KO mice (168.77±4.44 mg/dl); t_{33}= 3.869, $p<0.001$) comparisons were done expressing the results as percent of the concentration of glucose at time 0 of each corresponding mouse. For a better understanding, only the significant differences at basal levels are marked in figure 7.

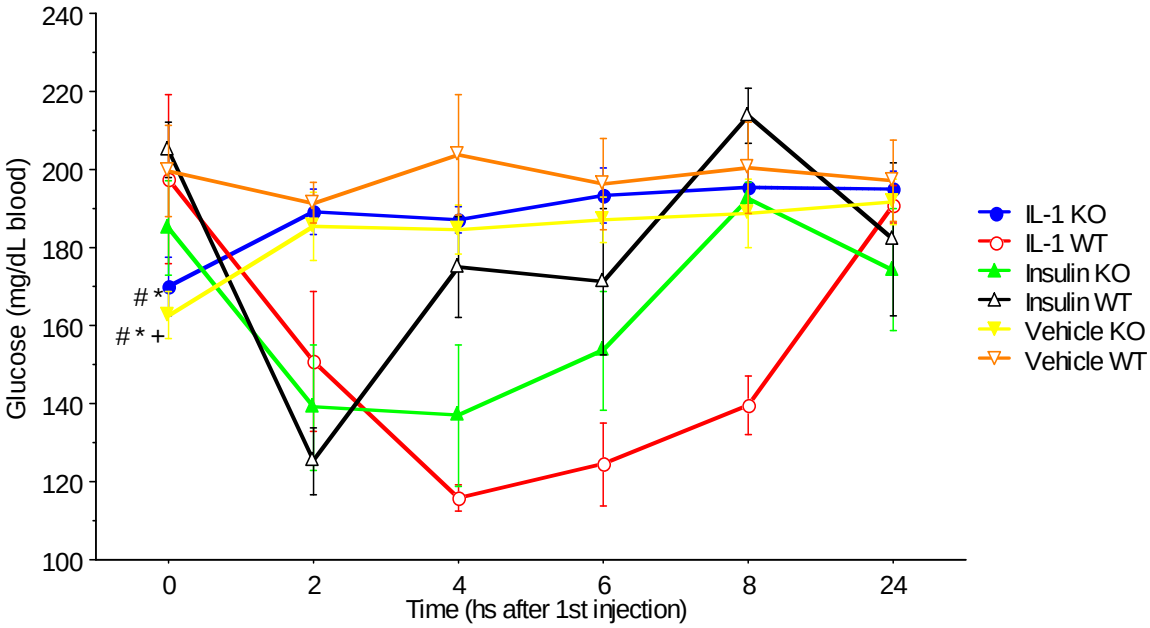

Figure 7 Effect of IL-1β on glucose levels. MyD88 KO and C57 BL/6J (WT) mice were randomized into 6 experimental groups: MyD88 KO mice received IL-1β (n=9), insulin (n=3) or vehicle alone (n=10). Correspondingly, WT mice received IL-1β (n=4), insulin (n=4), or vehicle alone (n=5). Blood glucose was measured at the times indicated in the curves. Each point in the curve represents the means ± SEM of the determinations performed in the number of the mice per group mentioned above. #p<0.05 vs. vehicle WT, *p<0.05 vs. Insulin WT, +p<0.05 vs. IL-1 WT

Confirming previous observations, IL-1β induced a profound and long-lasting hypoglycemia in WT mice. The levels of glucose in mice that received IL-1 were significantly lower than in vehicle-injected mice at times 2, 4, 6 and 8 hours after injection (Figure 8A). Insulin-injected WT mice showed significantly lower blood glucose levels than vehicle injected animals only at time 2. No significant differences were observed thereafter (Figure 8A).

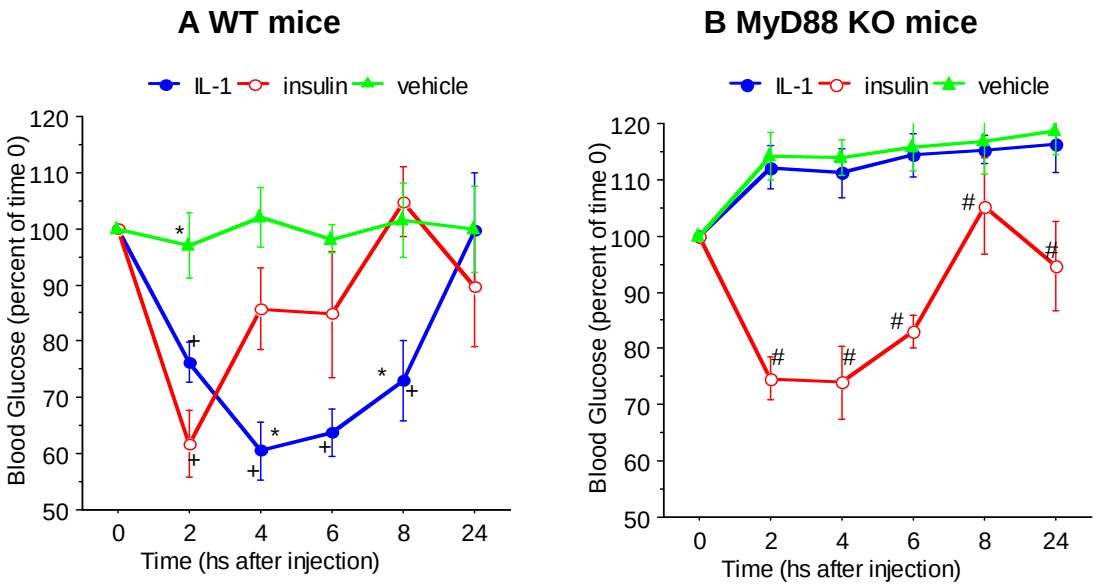

Figure 8 Effect of IL-1 on glucose levels in WT mice (Panel A) and MyD88 KO mice (Panel B). Blood glucose was measured at the times indicated in the curves. Results are expressed as percent of the corresponding time 0 for each individual mouse. Each point in the curves represents the mean ± SEM of the determinations performed in the number of mice per group indicated in the legend of Figure 7. + p<0.05 vs. vehicle *p<0.05 vs. insulin, # p<0.05 vs. IL-1 and vehicle

Conversely, IL-1β did not induce hypoglycemia in MyD88 KO mice (Figure 8B). Insulin injection in MyD88 KO mice resulted in a decrease in blood glucose levels at times 2, 4, 6 and 24 (Figure 8B). All 6 groups are shown superimposed in one graph in figure 9, in which only the statistically significant differences between the two genotypes that received the same treatment, are indicated. IL-1β-injected WT animals showed a statistically significant decrease in blood glucose as compared to IL-1β- injected MyD88 KO animals 2, 4, 6 and 8 hours after injection. There were no significant differences in glucose blood levels between MyD88 KO and WT mice following insulin injection. Vehicle-injected MyD88 KO animals showed statistically significantly increased blood glucose levels compared to vehicle-injected C57BL/6J mice 2, and 6 hours after injection when results are expressed as percent of their corresponding time 0. When the means of the absolute glucose values of these two groups are compared, there is only a difference at time 0 (independent sample t-test: t_{13}=3.163, p=0.007). There are no significant differences at any other time between vehicle-injected WT and MyD88KO animals. These results clearly show that IL-1β-induced hypoglycemia is MyD88-dependent.

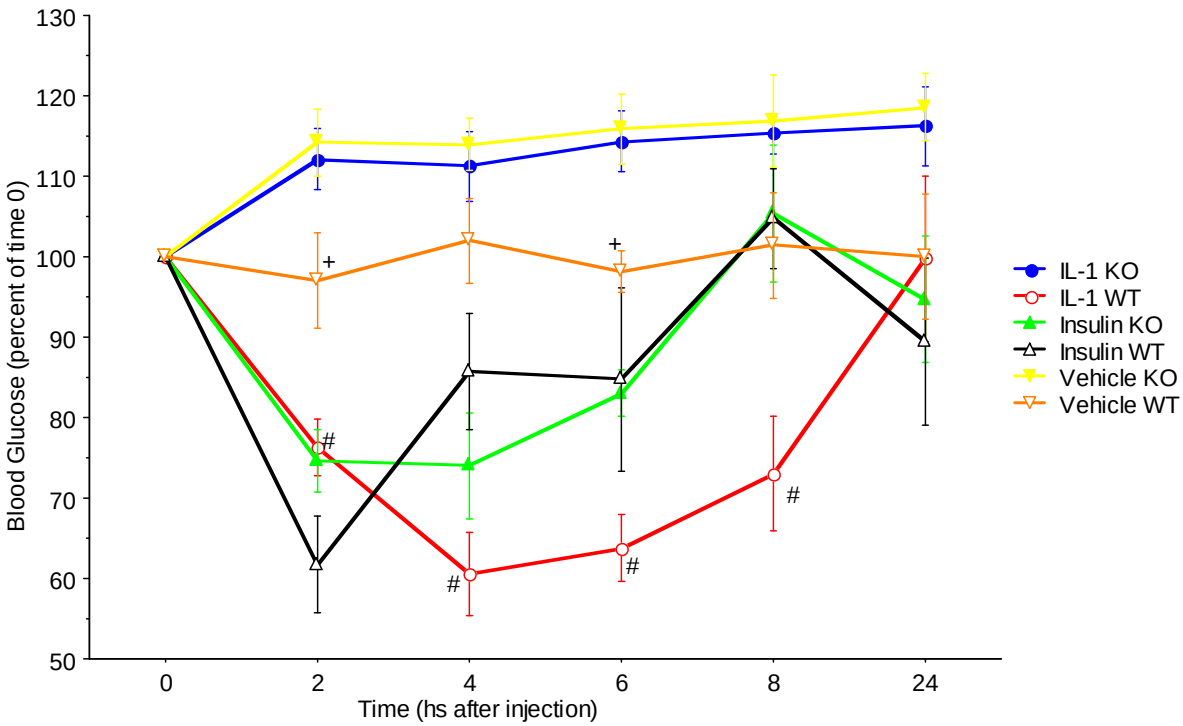

Figure 9 Blood glucose levels, expressed as percentage of time 0, following IL-1 or insulin injection into WT and MyD88 KO mice. The Results are expressed as percent of the glucose concentration determined at time 0 for each individual mouse. Each point in the curves represents the mean ± SEM of the determinations performed in the number of mice per group indicated in the legend of Figure 7. Since the groups differed significantly in the absolute basal blood glucose concentration, comparisons were done with the results expressed as percentage of their corresponding time 0 values. Only statistically significant differences between the groups that received the same injection are shown. # $p<0.05$ vs IL-1 KO; + $p<0.05$ vs vehicle KO

3.1.2 No effect of IL-1β on corticosterone blood levels in MyD88 KO mice

To explore if the effect of IL-1β on the HPA axis is also dependent on MyD88 signalling, corticosterone plasma levels were determined in the same groups of animals mentioned above. Confirming previous observations, IL-1β-injected C57BL/6J animals showed a marked increase in plasma corticosterone levels, as compared to vehicle- and insulin-injected animals 2, 4 and 6 hours after injection (figure 10A). Insulin-injected WT mice showed significantly higher blood corticosterone levels 2 hours after injection as compared to vehicle-injected WT mice (figure 10A). Plasma corticosterone levels in IL-1β-injected MyD88 KO mice did not differ from those of MyD88 KO animals that received insulin- or vehicle-injection (Figure 10B).

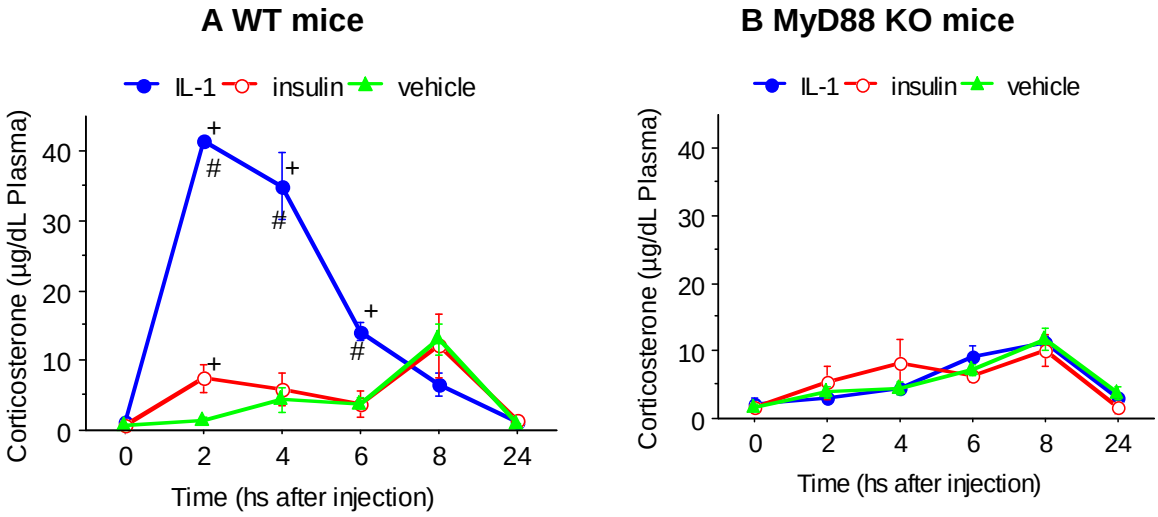

Figure 10 Effect of IL-1β on plasma corticosterone levels in C57BL/6J mice (Panel A) and MyD88 KO mice (Panel B). Corticosterone concentrations were determined by ELISA in plasma of the same mice as shown in Figure 7. Each point in the curves represents the mean ± SEM of the determinations performed in the number of the mice per group mentioned in the legend of figure 7. # p<0.05 vs. insulin; + p<0.05 vs. Vehicle

For better comparison, the plasma corticosterone concentrations of the animals of both genotypes that received the same treatment are shown in figure 11. There was no difference in corticosterone plasma levels between insulin-injected WT and KO mice or between vehicle-injected WT and KO mice at any of the time points studied (Figure 11A and B). IL-1β-injected WT animals showed statistically

significant higher corticosterone plasma levels than IL-1β-injected MyD88 KO animals 2, 4 and 6 hours after injection (Figure 11C).

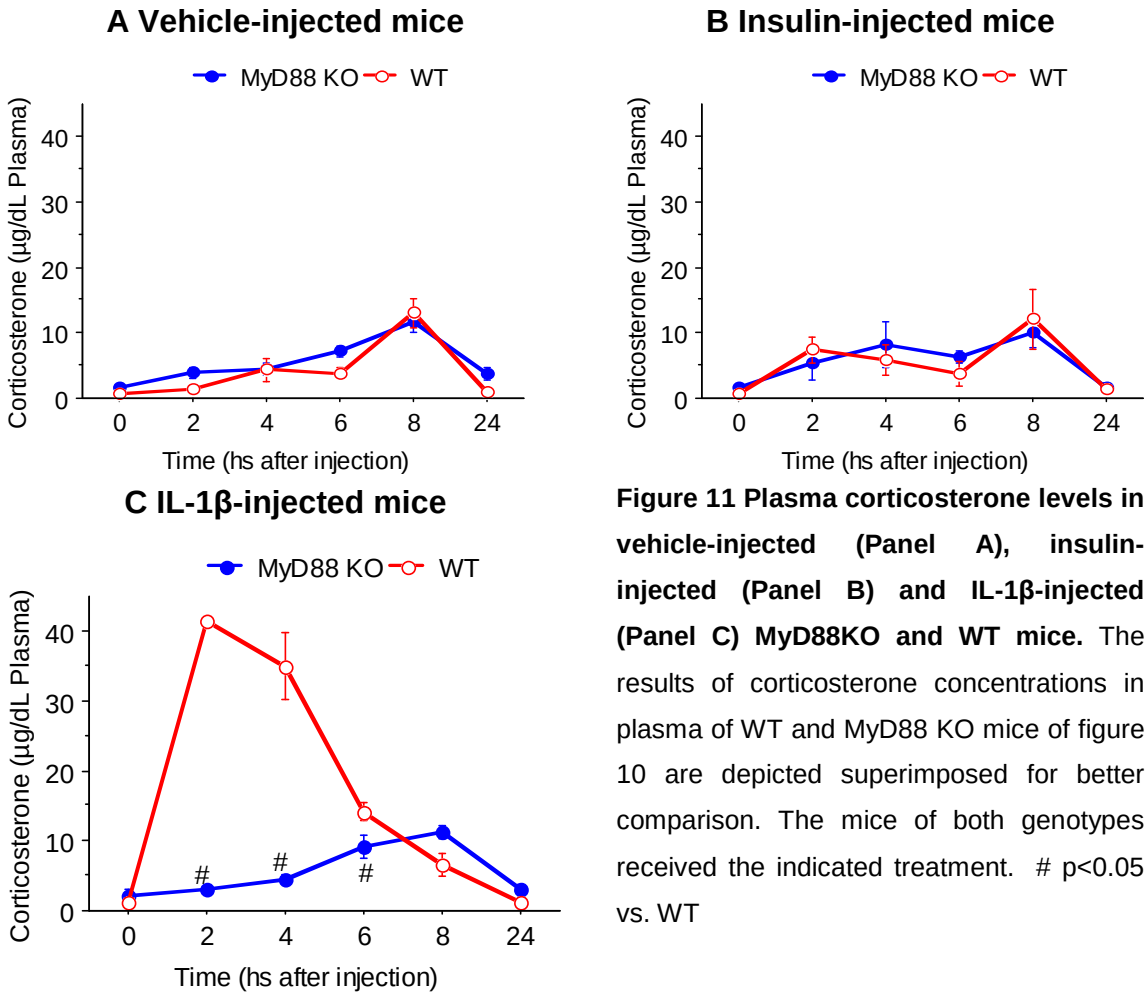

Figure 11 Plasma corticosterone levels in vehicle-injected (Panel A), insulin-injected (Panel B) and IL-1β-injected (Panel C) MyD88KO and WT mice. The results of corticosterone concentrations in plasma of WT and MyD88 KO mice of figure 10 are depicted superimposed for better comparison. The mice of both genotypes received the indicated treatment. # $p<0.05$ vs. WT

3.2 Pharmacological inhibition of MyD88 signalling does not influence IL-1β-induced hypoglycemia, but affects basal glucose levels

This experiment was designed to examine if pharmacological inhibition of MyD88 signalling could prevent the changes in glucose and corticosterone plasma levels induced by IL-1β. C57 BL/6J mice received the MyD88 inhibitor IMG2005 injected i.p. one hour prior to i.p. IL-1β injection, as proposed by the protocol of Van Tassell et al. (Van Tassell et al., 2010), and IL-6 plasma levels were determined 4 hours after IL-1β injection. The non-inhibiting control peptide was injected as control.

3.2.1 IMG2005 injection does not affect IL-6 levels

As described, the design of this experiment followed the protocol of Van Tassel et al. (Van Tassell et al., 2010). In this publication, IL-6 production was used as a surrogate to evaluate the effect of MyD88 inhibition by IMG2005 on IL-1-mediated effects. Thus, to control if MyD88 inhibition was successful, IL-6 levels in plasma were determined 4 hours after injection of the control peptide or the inhibitor and three hours after IL-1β-injection. The results obtained in the experiments performed in this work failed to reproduce the effect of IMG2005 reported by Van Tassell (IL-6 concentration (ng/dl): control peptide + IL-1β: 0.63 ± 0.34; n=4; Inhibitor + IL-1β: 0.41 ± 0.34 ng/dl; n=4). An independent sample *t*-test showed no statistically significant difference in the IL-6 concentration in plasma between the two groups (t_6=-0.597, p=0.573).

3.2.2 IMG2005 affects basal glucose concentrations but not IL-1β-induced hypoglycemia

Figure 12 shows absolute blood glucose values of WT mice that received the treatments described. Basal glucose levels differed significantly between the various groups (Figure 12, time 0). Due to the design of the experiment it was not possible to detect the significance of the difference during the experiment. Thus, a re-distribution of the animals to abolish the difference at basal levels was not possible. Therefore, glucose concentrations were calculated as percent of the basal concentration in each individual mouse.

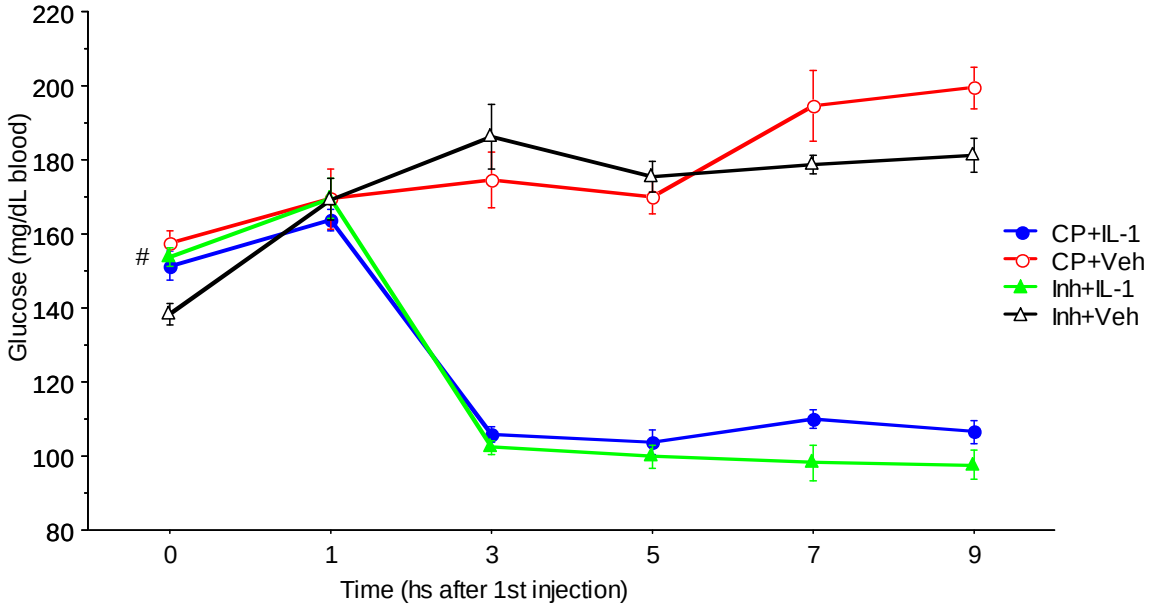

Figure 12 Blood glucose levels in IMG2005- and IL-1β-injected animals. C57 BL/6J mice were randomised into the following groups: IMG2005 and IL-1β (Inh+IL-1, n=11), IMG2005 and vehicle

(Inh+Veh, n=7), control peptide and IL-1β (CP+IL-1, n=11), control peptide and vehicle (CP+Veh, n=7). After collecting blood and determining blood glucose, animals received either IMG2005 or control peptide i.p. One hour later, after collecting blood and determining blood glucose concentrations, animals received IL-1β or vehicle also injected i.p. Additional blood samples were collected at the times indicated in the figure and glucose was determined. Each point in the curves represents the mean blood glucose concentration ± SEM determined in the number of animals mentioned above. The inh + veh group showed a statistically significant lower basal blood glucose concentration as compared to all the other groups. # <0.05 vs Inh + Veh

Blood glucose levels decreased markedly following IL-1β injection into mice that received control peptide, as well as in those that received the inhibitor (Figure 13) and animals in both groups developed a statistically significant hypoglycemia after IL-1β injection as compared to their corresponding controls. This hypoglycemia was still observed 9 hours after the first injection, i.e. 8 hours after IL-1β injection. There was no significant difference between the CP + IL-1β group and the Inh + IL-1β group when results were calculated as percent of the basal levels. However, 3 and 5 hours after the first injection, mice that received the inhibitor and vehicle alone (inh + veh) developed a statistically significant hyperglycaemia compared to mice that received the control peptide and vehicle alone (CP + veh). No significant differences between these two groups were detected at later time points (Figure 13).

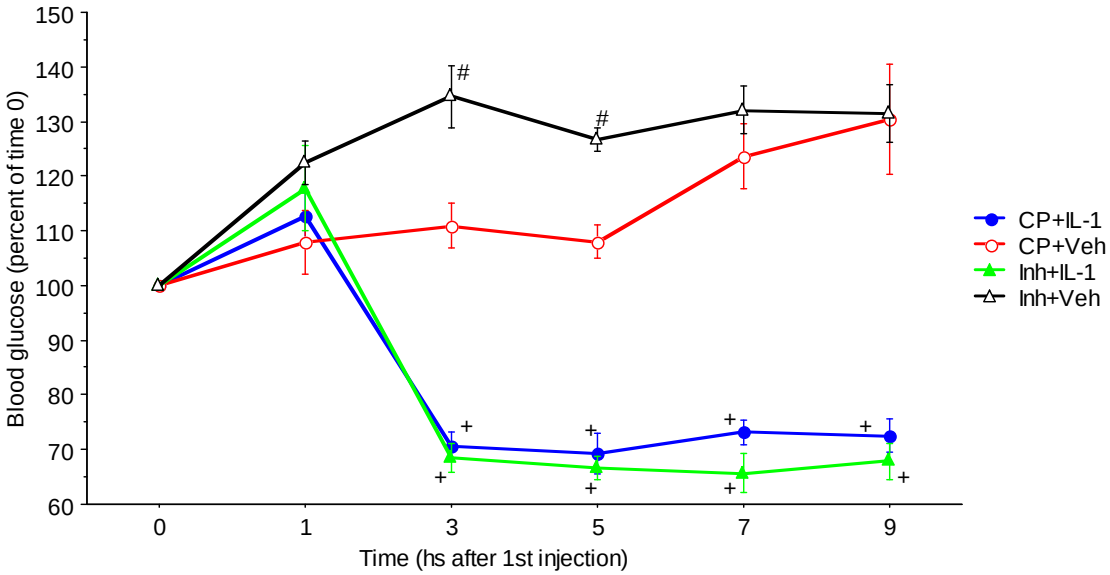

Figure 13 Effect of IMG2005 on blood glucose of IL-1β and vehicle-injected WT mice. Animals were randomized into the groups indicated in the legend of Figure 12. After determining basal glucose values, mice were injected i.p. either with IMG2005 or with the control peptide. One hour later glucose values were determined again and either IL-1β or vehicle was injected i.p. Each

point in the curve represents the mean of blood glucose concentrations calculated as percent of the time 0 ± SEM of each individual animal. # p<0.05 vs. CP+Veh + p<0.05 vs Inh+Veh and CP+Veh

3.2.3 IMG2005 does not influence plasma corticosterone levels

As can be seen in figure 14, prior treatment with IMG2005 did not result in statistically significant differences in the concentration of corticosterone in plasma of animals that received vehicle nor the elevation in corticosterone levels induced by IL-1 administration, at any of the time points studied.

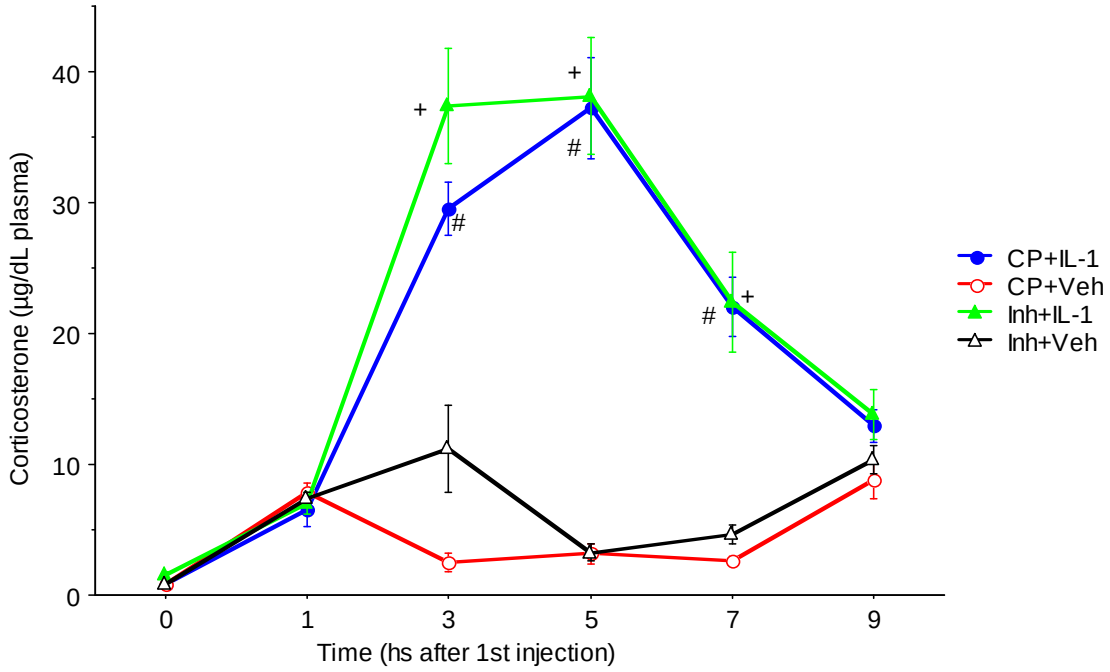

Figure 14 Influence of IMG2005 administration on blood corticosterone levels. C57BL/6J animals were randomised into the groups as indicated in figure 16. The group size was 7 for all groups, since the plasma of two mice of each inhibitor-injected group was used for IL-6 determination. Blood was collected at the times indicated above and corticosterone determined with an ELISA. Each point in the curve represents the means of plasma corticosterone concentration ± SEM determined in the respective group. # p<0.05 vs. CP+Veh +p<0.05 vs Inh+Veh

3.3 IL-1β injection affects brain energy metabolism

The objective of these experiments was to investigate the *in vivo* effect of IL-1β on brain energy metabolism, and to compare it with that of insulin. Therefore cerebral magnetic resonance spectroscopy for semi-quantitative determination of Cre, Lac and NAA in relation to Cho was performed in groups of mice that received either

the vehicle alone, IL-1β or insulin. Additionally, glucose and corticosterone concentrations in blood were determined before and after each MRS scan.

3.3.1 Changes in blood glucose concentrations after insulin and vehicle injection but not after IL-1β injection during the MRS procedure

Two hours after injecting IL-1β (0.1 µg) or insulin (4 U/kg b.w.) and immediately before the second MRS determination, blood glucose levels significantly differed from those of the mice that received the vehicle alone (Figure 15A). To keep insulin induced-hypoglycemia at comparable glucose levels to that of IL-1β-induced hypoglycemia, a second injection of insulin was necessary four hours after the first one. The same degree of hypoglycemia was also observed in IL-1- and insulin-injected mice at later time points (4, 6 and 8 hours) when glucose levels were evaluated before performing the corresponding MRS determination. However, when glucose levels were determined immediately after each MRS scan (which implied ca. 35 minutes of isoflurane narcosis) it was evident that the insulin-injected animals had a more profound hypoglycemia than those mice that had received IL-1 (figure 15B).

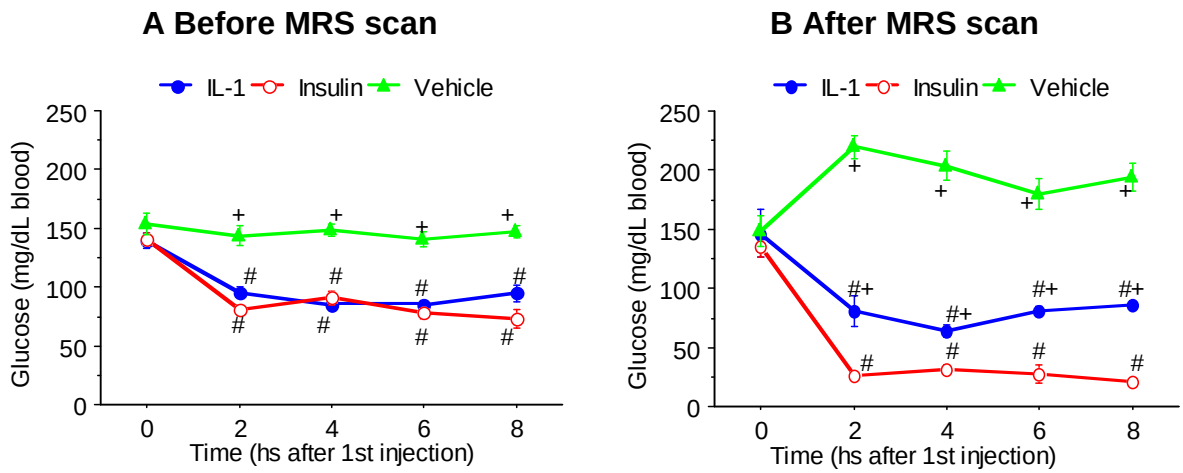

Figure 15 Blood glucose of IL-1-, insulin- and vehicle injected animals before (Panel A) and after (Panel B) each MRS scan. Blood samples were collected and glucose determined before a basal cerebral MRS scan was performed (time 0). A second determination of glucose levels and blood collection was performed immediately after MRS data were acquired, and animals received randomly either IL-1β (n=7), insulin (n=9) or vehicle (n=9) injected i.p. Further scans followed as described in 2.5.3. Blood was collected and glucose determined directly before and after each scan. Each point in the curve represents the mean blood glucose levels ± SEM. Two hours after

IL-1β- and insulin administration, and before every MRS scan, animals showed hypoglycemia as compared to vehicle-injected animals (Panel A). Blood glucose values after MRS scan differed statistically significantly between all three groups. Vehicle-injected animals showed hyperglycaemic levels, whereas mice of the IL-1β group showed hypoglycaemic values. Even lower glucose values could be detected in insulin-injected animals (Panel B). # p<0.05 vs. vehicle; + p<0.05 vs. insulin

The comparison of glucose concentrations before and after MRS determinations showed that blood glucose statistically significantly increased in the control group (figure 16A), while it decreased in insulin-injected animals (figure 16B) and did not change in the IL-1β-injected group (figure 16C) during 35 minutes of MRS procedure.

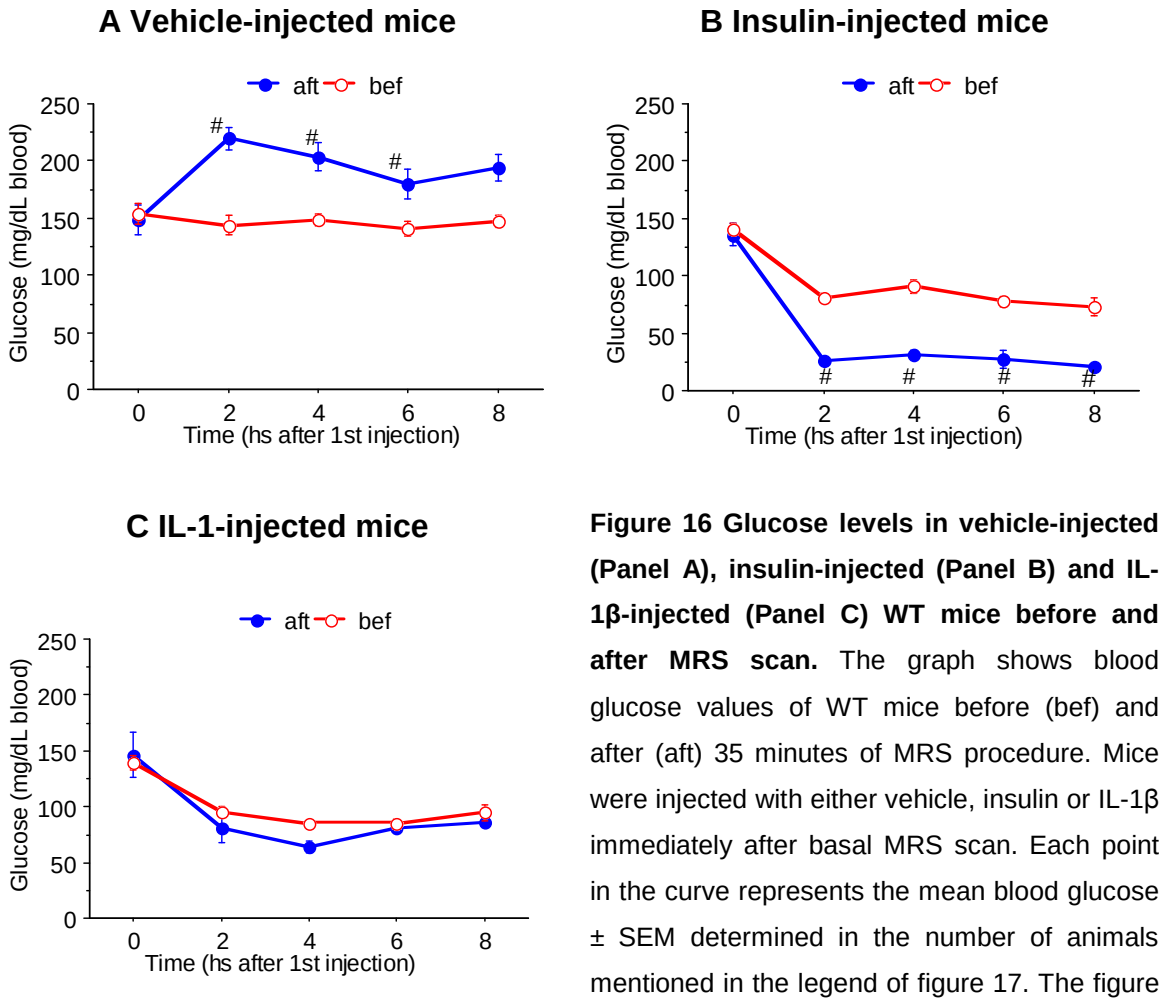

Figure 16 Glucose levels in vehicle-injected (Panel A), insulin-injected (Panel B) and IL-1β-injected (Panel C) WT mice before and after MRS scan. The graph shows blood glucose values of WT mice before (bef) and after (aft) 35 minutes of MRS procedure. Mice were injected with either vehicle, insulin or IL-1β immediately after basal MRS scan. Each point in the curve represents the mean blood glucose ± SEM determined in the number of animals mentioned in the legend of figure 17. The figure shows that blood glucose concentrations of vehicle-injected mice increased (Panel A), whereas those of insulin-injected animals decreased (Panel B) and those of IL-1β-injected mice were not influenced (Panel C) during 35

minutes of MRS procedure. # p<0.05 vs. bef

To control if the decrease of blood glucose levels in insulin-induced hypoglycemia during the 35 minutes of MRS acquisition was caused by isoflurane narcosis, a separate group of animals was subject to 35 minutes of isoflurane narcosis, following exactly the same procedure but without MRS recording. Blood glucose was determined before and after narcosis and the procedure was repeated four times, at intervals of two hours.

Figure 17 shows glucose concentrations in blood of vehicle- and insulin-injected mice respectively, before and after narcosis. Vehicle-injected mice showed hyperglycaemic levels after 35 minutes of narcosis, whereas a further decrease in blood glucose concentrations could be observed following the same procedure 4 and 6 hours after insulin injection. Although only 3 mice per group were included, the effect of the narcosis was statistically significant. It was concluded that the changes in glucose blood levels observed during the scans were not due to the MRS procedure but rather to the narcosis itself.

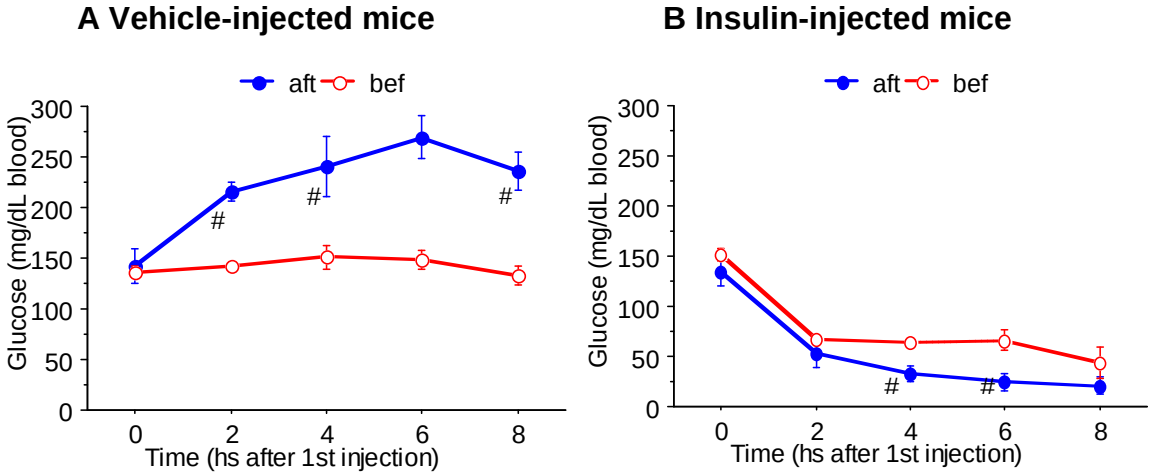

Figure 17 Blood glucose of vehicle-injected mice after 35 minutes of isoflurane narcosis

C57 BL6/J animals were randomized into a vehicle-injected control group (n=3) and an insulin-injected group (n=3). Blood glucose was determined and animals underwent 35 minutes of isoflurane narcosis. Afterwards blood glucose was determined again. This procedure was repeated 4 times, at intervals of two hours. This figure shows blood glucose values before narcosis (bef) compared to those after narcosis (aft) of vehicle-injected (Panel A) and insulin-injected (Panel B) mice. Each point in the curves represents the mean blood glucose levels ± SEM. Blood glucose values of vehicle injected animals increase statistically significantly after 35 minutes of narcosis, whereas those of insulin-injected animals decreased after narcosis 4 and 6 hours after the first insulin-injection. # p< 0.05 vs. bef

3.3.2 Plasma corticosterone concentrations increase during the MRS scan

Plasma corticosterone levels significantly increased after IL-1β injection as compared to those of insulin- or vehicle-injected animals. This effect was observed before (figure 18A) as well as after (figure 18B) each MRS with exception of the last MRS scan, after which there was no statistical significant difference between the groups.

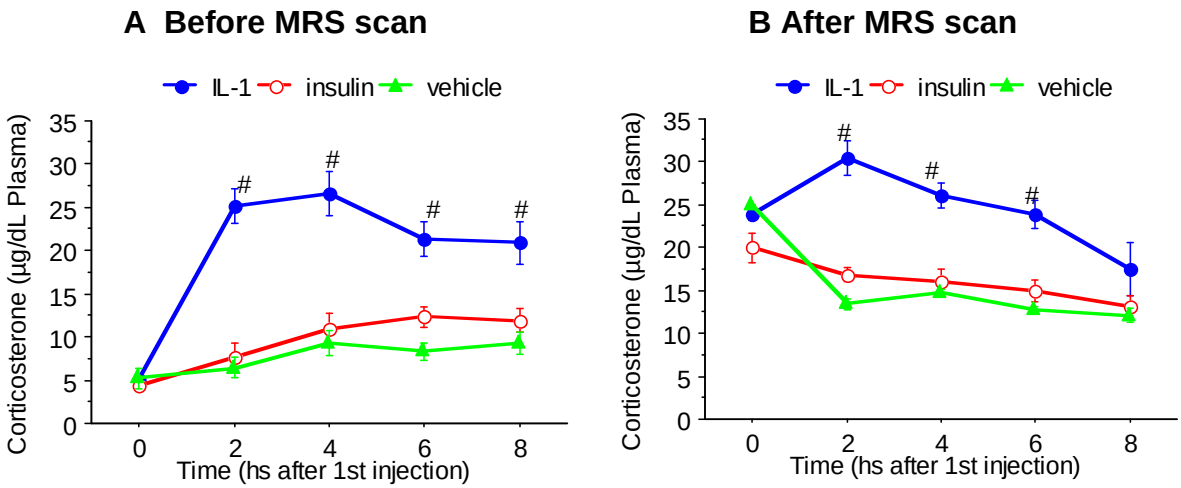

Figure 18 Plasma corticosterone levels before (Panel A) and after (Panel B) MRS scan. Plasma corticosterone levels were determined in the same mice as used for glucose determinations. As indicated in figure 15 these animals received either IL-1β (n=7), insulin (n=9) or vehicle (n=9) i.p. Blood was collected before and after each MRS scan. The graph shows plasma corticosterone levels before (panel A) and after (panel B) MRS scans. Plasma corticosterone concentration was determined by ELISA. Each point in the curve represents the mean plasma corticosterone ± SEM. IL-1β-injected animals showed increased plasma corticosterone levels after MRS at every time after injection, apart from the last MRS scan performed. # $p<0.05$ vs. Insulin and Control

When comparing corticosterone levels before and after MRS during the first scan, it can be observed that corticosterone levels increased in all groups during the MRS procedure. This rise becomes less prominent with each following MRS scan and it is no longer statistically significant at time 8 in the mice that received vehicle (figure 19A), at time 6 in the insulin-injected group (figure 19B) and at time 4 in mice that received IL-1β (figure 19C).

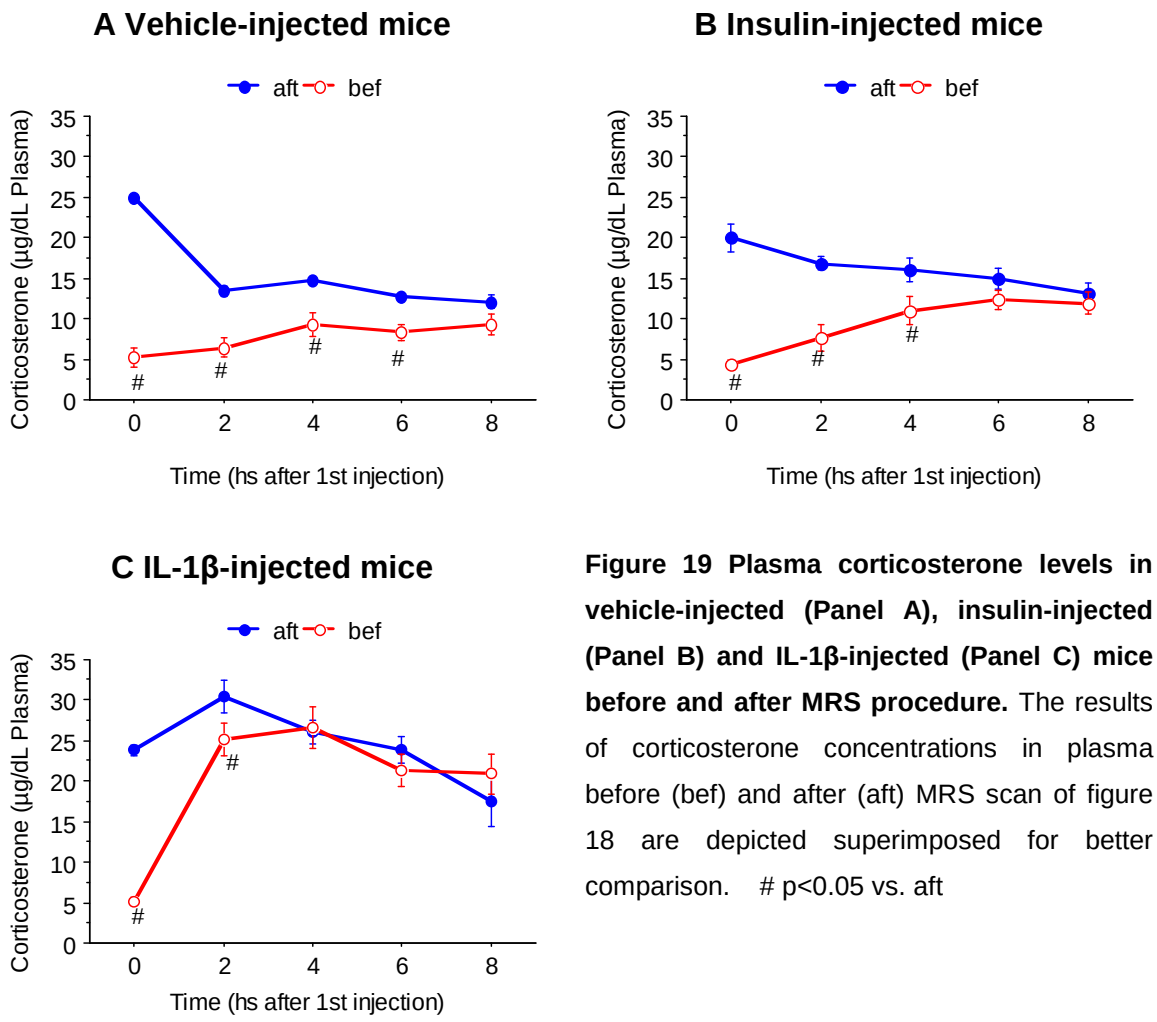

Figure 19 Plasma corticosterone levels in vehicle-injected (Panel A), insulin-injected (Panel B) and IL-1β-injected (Panel C) mice before and after MRS procedure. The results of corticosterone concentrations in plasma before (bef) and after (aft) MRS scan of figure 18 are depicted superimposed for better comparison. # $p<0.05$ vs. aft

3.3.3 Differences in brain metabolites between IL-1β-, Insulin- and vehicle-injected animals

To evaluate brain energy metabolism under the influence of IL-1β, MRS brain scans were performed, as described in chapter 2.3.6. NAA, Cre, Lac and Cho were identified in the spectra. Figure 20 shows an example of the spectrum obtained before any injection (time 0). The integrals of the peaks are proportional to the concentration of the corresponding metabolite. To avoid deviations due to possible changes in the magnetic field, the metabolites are commonly divided by the integral of the Cre peak. However, since creatine levels may be affected by changes in energy metabolism, Cho was used as reference because it is not considered to be altered during changes in energy metabolism.

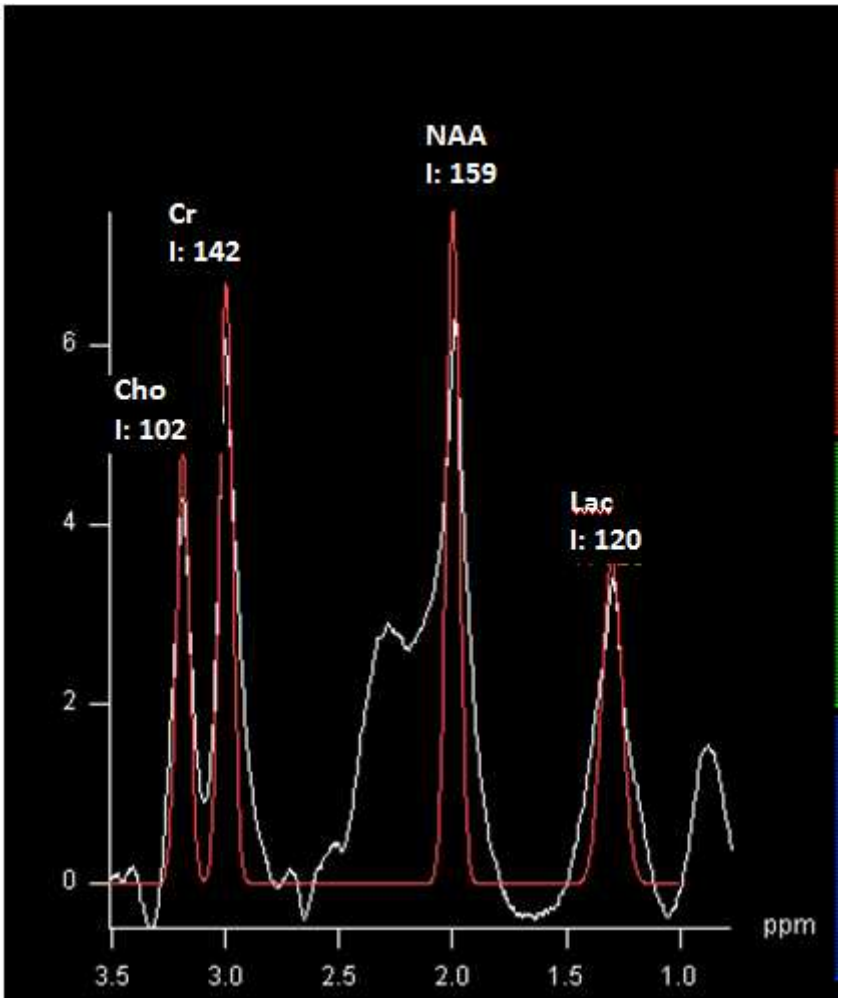

Figure 20 Example of an MR spectrum obtained from a non-injected mouse. The white line represents the spectrum acquired and the red line indicates the corresponding curve-fit. I: Integral

The ratios NAA/Cho, Cre/Cho and Lac/Cho did not statistically differ between the mice assigned to the different treatment groups.

The difference between NAA/Cho, Cre/Cho and Lac/Cho ratios at each time point and the corresponding ratio at time 0 for each individual mouse was used for further statistical analyses.

Mice of the IL-1β-treated group showed a significantly increased NAA/Cho ratio relative to their initial values at 8 hours as compared to those of the insulin group. In the insulin-treated group this difference was negative and statistically decreased as compared to the difference of the NAA/Cho ratio relative to initial values in the control group (figure 21).

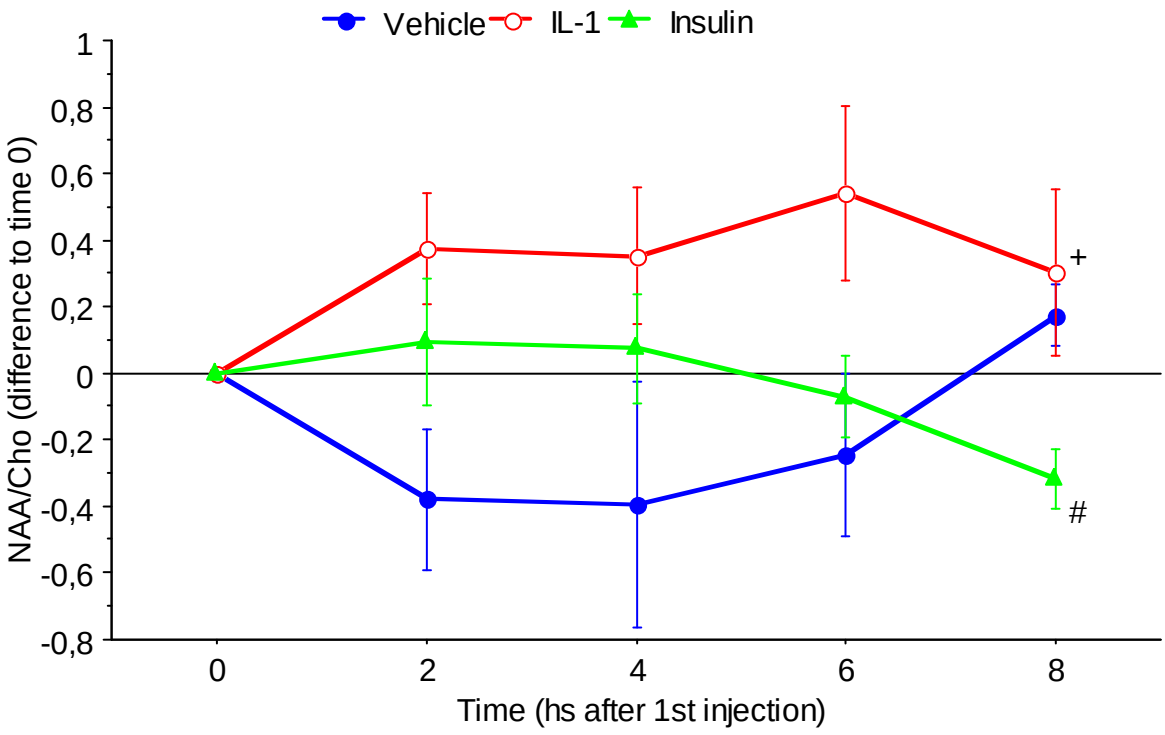

Figure 21 Changes in the differences in NAA/Cho ratios after IL-1, insulin and vehicle injection. C57BL/6J animals were randomised into 3 groups as mentioned in figure 18. MRS was obtained as described in 2.3.6. The MRS obtained before any injection was defined as basal determination (time 0). Each point in the curves represents the mean ± SEM of the difference between the NAA/Cho ratio at a given time and the ratio at time 0 for each individual mouse. # $p<0.05$ vs. vehicle, + $p<0.05$ vs. insulin

Regarding Cre, the differences in the Cre/Cho ratios were significantly increased in the IL-1β-treated group at 4 and 6 hours as compared to the control group and at 6 and 8 hours as compared to the insulin-treated group (Figure 24).

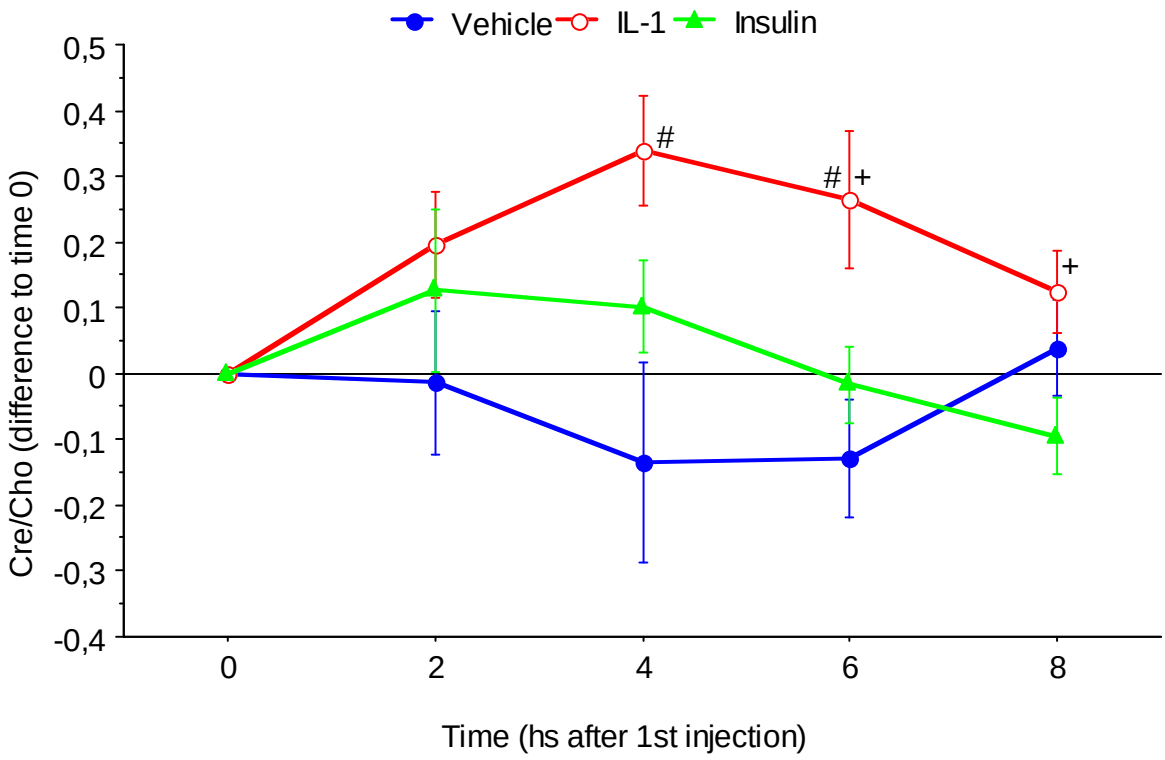

Figure 22 Changes in the difference of Cre/Cho ratios after IL-1, insulin and vehicle injection. As described in legend to figure 21, but showing the Cre/Cho ratio at a given time and the ratio at time 0 for each individual mouse. Each point in the curve represents the mean ± SEM # $p<0.05$ vs. vehicle, + $p<0.05$ vs. insulin

The differences in the Lac/Cho ratios were significantly higher in IL-1β-treated mice as compared to those of the vehicle-injected mice 6 hours after injection (figure 23).

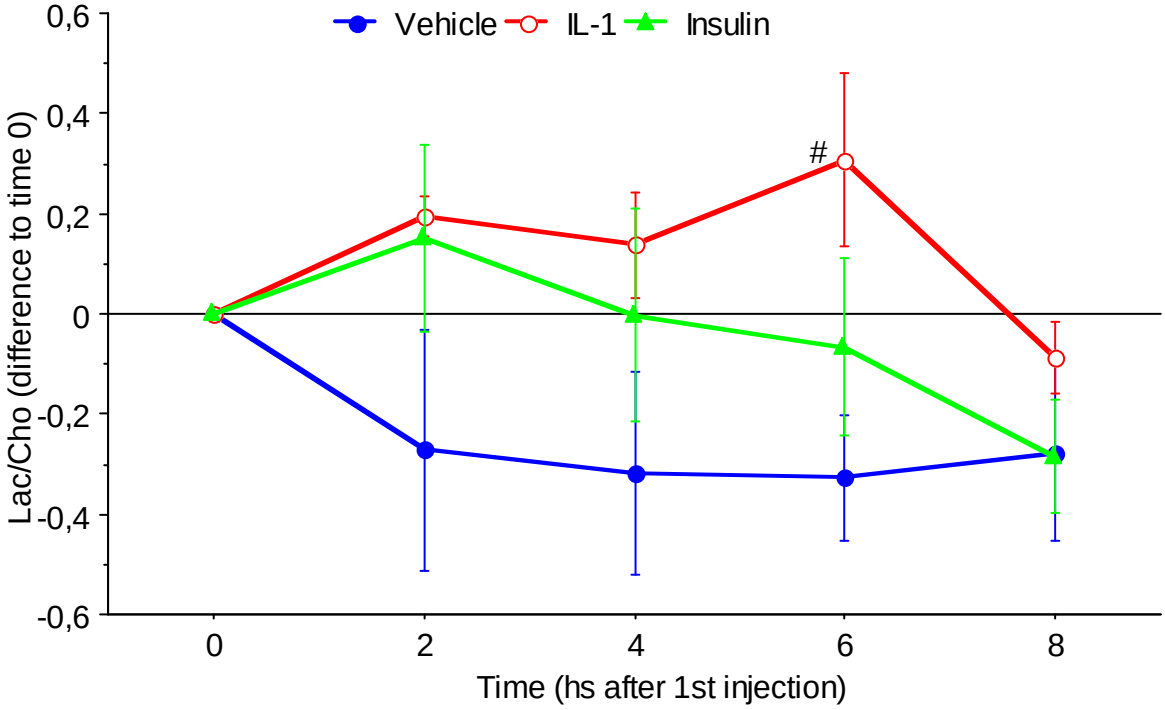

Figure 23 Changes in the difference of Lac/Cho ratios after IL-1, insulin and vehicle injection. As described in legend to Figure 21, but showing the Lac/Cho ratio at a given time and the ratio at time 0 for each individual mouse. Each point in the curves represents the mean ± SEM. # $p<0.05$ vs. vehicle

In conclusion, the differences in the ratios NAA/Cho, Cre/Cho and Lac/Cho were in general elevated in IL-1β-injected mice as compared to those of vehicle- and/or insulin-injected animals. These differences were statistically significant between 4 and 6 hours after injection, and in part were still detectable after 8 hours.

4 DISCUSSION

4.1 IL-1β-induced hypoglycemia and the stimulation of the HPA-axis depend on MyD88-mediated signalling

As shown in chapter 3.1.1, IL-1β-induced hypoglycemia is dependent on mechanisms that function via MyD88 signalling. Confirming previous results, IL-1β injection into C57BL/6J resulted in a profound hypoglycemia and in the stimulation of the HPA axis (del Rey and Besedovsky, 1987; del Rey and Besedovsky, 1992; del Rey et al., 2006). However, neither hypoglycemia nor increased corticosterone levels were observed after IL-1β administration into MyD88-deficient mice. These results clearly show that the mentioned effects of IL-1β are mediated by this universal adapter protein. As explained in chapter 1.2.4, it remains still unclear to what extent peripheral and cerebral effects contribute to IL-1β-induced hypoglycemia. Also, the signalling mechanisms that are involved in the effects that IL-1β exerts at brain levels are still controversial (Dantzer, 2009). It is therefore possible that the central effect of IL-1β that results in hypoglycemia is itself not MyD88-dependent, but its transmission across the blood-brain-barrier (BBB). To further elucidate this question, A. Lörwald showed in her diploma thesis that i.c.v. injection of 5ng of IL-1β induces hypoglycemia in heterozygous MyD88$^{+/-}$ animals but not in MyD88 KO animals (Lörwald, 2012), thus providing first evidence that MyD88 in the brain is essential for direct effects of IL-1-induced hypoglycemia. Confirming the results of former studies (Gosselin and Rivest, 2008; Ogimoto et al., 2006), no increase in corticosterone plasma levels were observed in MyD88 KO mice. It cannot be excluded that the response of the HPA axis in MyD88 KO animals is impaired due to general impossibility to release corticosterone beyond a certain level in these animals. However, this seems to be unlikely for various reasons: a) Vehicle-injected MyD88 KO mice showed no significant different corticosterone plasma levels when compared to WT mice. B) Corticosterone plasma levels showed the typical circadian rhythm in both KO and WT mice. Since cerebral MyD88 expression is necessary for the hypoglycaemic effects of IL-1β, the same might apply for the activation of the HPA-axis (Gosselin and Rivest, 2008).

The results derived from the pharmacological inhibition of MyD88 are less clear. There are very few MyD88 inhibitors available, and IMG2005, the inhibitor used in the studies reported here, did not abrogate the effects of IL-1β at the concentration administered. It has been reported that the same concentration of IMG2005 as used in the studies shown here can inhibit IL-6 production and cardial dilatation after ischemia (Van Tassell et al., 2010). However, neither IL-6 release nor IL-1β-induced hypoglycemia or the activation of the HPA axis were influenced by this inhibitor in our studies. As described in this work and by others as well, corticosterone blood levels do not increase after IL-1β injection into MyD88 KO mice (Gosselin and Rivest, 2008; Ogimoto et al., 2006). However, Ogimoto et al. demonstrated that MyD88 KO mice show IL-6 and IL-10 levels comparable to those of WT mice after LPS injection. Thus, it is possible that IL-1-induced IL-6 production is not, or not alone, dependent on MyD88. Furthermore, it is possible that the dose of IL-1β applied was too high in relation to the IMG2005 dose. Since stimulation of very few IL-1RI is enough to activate intracellular signalling (Stylianou et al., 1992), almost all TIR domains of IL-1RI-IL-1RacP complexes must be blocked in order to inhibit IL-1β signalling effectively. (Ogimoto et al., 2006)

However, it is noteworthy that injection of the inhibitor alone resulted in hyperglycaemia 3 and 5 hours after administration. This indicates that MyD88-signalling may play a role in basal glucose homeostasis under physiological, healthy conditions. In support of this possibility are other studies showing that IMG2005 injected i.c.v. causes an even more marked hyperglycaemia (Lörwald, 2012). Thus, further experiments with higher doses of IMG2005 injected peripherally or the use of other MyD88 inhibitors are needed to investigate the role of IL-1 or other members of the TIR-family on glucose regulation under physiological conditions.

The same considerations apply to the lacking of effect of IMG2005 administration on IL-1β-induced increase in corticosterone levels. As expected, IL-1β injection resulted in statistically significant increased corticosterone blood levels as compared to vehicle-injected animals, but IMG2005 did not block this effect. Experiments using higher concentrations of IMG2005, injected i.p. and i.c.v. are necessary to further investigate the involvement of MyD88 in IL-1β-induced activation of the HPA-axis.

4.2 Changes in glucose and corticosterone levels during MRS

The procedures needed to acquire the MRS data, including narcosis, induced an increase in glucose blood levels in vehicle-injected mice. Conversely, insulin-injected animals showed a further decrease in blood glucose concentration after exposure to approximately 35 minutes of MRS and isoflurane narcosis during the acquisition of the MRS data. To investigate if these effects were due to isoflurane inhalation, insulin- and control-injected animals received 35 minutes of isoflurane anaesthesia alone. This treatment resulted in effects comparable to those observed in mice that underwent MRS and narcosis. The increase in blood glucose levels observed in vehicle-injected mice is most likely caused by a stress response to the narcosis, blood collection and injection.

Furthermore, isoflurane has a pharmacologic effect on glucose metabolism. It has been reported that patients undergoing isoflurane narcosis show impaired insulin secretion and hyperglycaemia (Diltoer and Camu, 1988). Isoflurane increases blood glucose levels by decreasing the sensitivity of pancreatic K_{ATP}-channels to ATP, thus leading to hyperpolarisation and decreased insulin secretion after a glucose load (Tanaka et al., 2011). Furthermore, it has been shown that volatile halogenated anaesthetics lead to enhanced activation of K_{ATP}-channels in smooth muscle tissue and cardiomyocytes during decreased intracellular ATP concentration (Fujimoto et al., 2002; Tanaka et al., 2007). However, it is not yet known how isoflurane interacts with cerebral K_{ATP}-channels or which effects are elicited in states of hypoglycemia. Since isoflurane crosses the BBB, it is possible that it has an effect on hypothalamic K_{ATP}-channels in GE-neurons, which are of the same subtype as pancreatic K_{ATP}-channels (Seino and Miki, 2003). If isoflurane leads to a relative hyperpolarisation of GE-neurons, as it does in pancreatic β-cells, this would lead to an increased hypoglycaemic counterregulation. As described in chapter 1.5, hyperpolarisation of hypothalamic GE-neurons leads to an increase of hypoglycaemic counterregulatory hormones. In our experiments, isoflurane application enhanced the hypoglycaemic effects of insulin resulting in very low blood glucose levels (30mg/dl or less). One possibility is that isoflurane impairs not only insulin release, but also interferes with counter regulatory mechanisms such as the release of monoamines, glucocorticoids or glucagon. Evidence exists that isoflurane might reduce adrenalin levels in humans (Diltoer and Camu, 1988) and that it does not influence glucagon levels

(Lattermann et al., 2003; Schricker et al., 2004). However, corticosterone levels were increased under isoflurane anaesthesia. Another possible explanation would be that isoflurane acts synergistically at the effector cells, mainly in skeletal muscle, fat and liver either by increasing the affinity of the insulin receptor to insulin or by enhancing anabolic effects of insulin.

A most interesting observation within the context of this work is that IL-1β-injected animals showed comparable levels of blood glucose before and after narcosis, although they were subjected to the same experimental procedure as those that received insulin or vehicle alone. These results provide a further argument in support of the hypothesis that IL-1β resets glucose homeostasis at a hypoglycaemic set-point, as discussed in chapter 1.2.4. The corticosterone levels of insulin- and vehicle-injected animals showed the largest increase after the first MRS scan. This is most likely an expression of a stress-induced activation of the HPA-axis. The increase in corticosterone blood levels during the MRS scans became gradually less pronounced during the course of the experiment until the difference of the corticosterone levels before MRS procedure compared to those after MRS procedure was no longer statistically significant after 6 hours. This is probably due to adaptation to the experimental procedure.

IL-1β-injected animals showed an increase in corticosterone levels during the first MRS scan. Elevated levels of corticosterone were also observed at the second MRS

scan, as expected, due to IL-1β-induced activation of the HPA-axis, which peaks 2

hours after injection and decreases thereafter. The increase in corticosterone concentration is limited by the capacity of the adrenal gland. Thus, corticosterone concentrations did not increase further at the third MRS scan.

4.3 IL-1β affects brain energy metabolism: differences with the effects of insulin

The main aim of these experiments was to evaluate cerebral energy metabolism under IL-1β-induced hypoglycemia and to compare it with the effects of a comparable hypoglycemia induced by insulin. It was not possible to detect glucose directly with the MRS device available, since the H^1 MR glucose signal is overlain by the water signal. Therefore Lac, Cre and NAA were used as

parameters to evaluate brain energy metabolism. Cho, the fourth metabolite determined, is not considered to play a role in neuronal energy metabolism and was therefore used as a reference. As discussed in chapter 1.4, Lac is a fuel for neurons, derived mainly from anaerobic glycolysis, whereas Cre and NAA contribute to support neuronal energy metabolism. Cre is involved in the phosphocreatine/creatine-kinase/creatine system that participates in the high energy phosphate metabolism of tissues with high and fluctuating energy demand (Bittsansky et al., 2012; Schwarcz et al., 2003; Wallimann et al., 1992; Wyss and Kaddurah-Daouk, 2000).

According to the classical view, ketone bodies and amino acids, such as glutamate and aspartate, are the main source of energy for the brain during severe insulin-induced hypoglycemia and hypoglycaemic coma (Agardh et al., 1978; Sutherland et al., 2008). However, there is evidence that during increased neuronal activity, energy consumption or hypoglycemia, astrocytes shuttle glucose-derived lactate or pyruvate to neurons to cope with the emerged fuel-gap (Brown and Ransom, 2007; Brown et al., 2005; Suh et al., 2007).

Regarding the changes in the metabolites evaluated from basal conditions until 8 hours after injection, IL-1β-injected mice showed an increase in all parameters measured as compared to vehicle-injected animals (Lac/Cho), insulin-injected animals (NAA/Cho) or both (Cre/Cho). The increase reached statistical significance 4-8 hours after injection. These results suggest that, under the influence of IL-1β, brain energy metabolism is enhanced even though blood glucose levels are decreased. A possible explanation for this effect is that IL-1β increases the availability of energy substrates to neurons, thus “hiding” the peripheral hypoglycemia to the brain. Most likely, this would be achieved by an increased neuronal uptake of either glucose, or lactate, or both. It has been previously shown, that the mechanisms that counterregulate hypoglycemia, as represented by increased plasma concentrations of corticosterone and glucagon are no longer observed 4 to 8 hours after IL-1β injection (del Rey and Besedovsky, 1987; Ota et al., 2009). This coincides with the time interval when the main differences in the metabolite ratios are observed in the experiments described here, thus providing further evidence to the hypothesis, that IL-1β-induced hypoglycemia is not detected by the brain. Furthermore, MyD88 KO mice,

which do not develop hypoglycemia after IL-1β injection, do not show changes in the metabolite ratios comparable to those of WT mice (Lörwald, 2012).

As mentioned in chapter 1.5, infusion of glucose or lactate in the hypothalamus induces hypoglycemia and inhibits hypoglycaemic counterregulation by changing the ADP/ATP-ratio in GE- and GI-neurons (Borg et al., 1997; Borg et al., 2003; Song and Routh, 2005). It has already been reported that IL-1β induces glucose uptake and utilization in astrocytes (Vega et al., 2002), but no data is available concerning neurons. It is also not known if IL-1β affects lactate metabolism in neuronal or glial cells. Another possibility would be that neurons take up lactate provided by astrocytes as proposed by the ANLS-hypothesis (see 1.4).

Since the concentrations of NAA and Cre rise in states of increased energetic metabolism (Bittsansky et al., 2012; Clark, 1998; Moffett et al., 2007; Wyss and Kaddurah-Daouk, 2000), the relative Cre and NAA increase might reflect an indirect effect of IL-1 due to an increased energy metabolism.

Interestingly, no comparable differences were detected in the metabolites between insulin- and vehicle-injected animals. It could have been expected that cerebral lactate concentration would decrease under insulin-induced hypoglycemia. In fact, Rao et al. showed that 60-80 minutes after initiation of insulin-induced hypoglycemia, brain lactate concentration decreases (Rao et al., 2010). However, these experiments were done with 14 day-old pups, which suffered a more profound hypoglycemia than the adult animals used in our experiments. It has also been reported that a decrease in cerebral lactate concentration can be first detected in the hippocampus of the young pups only after around 90 minutes of blood glucose values below 50mg/dl (Lewis et al., 1974; Rao et al., 2010) and in parallel to neuroglycopenia. In the experiments described here, the adult animals suffered a comparable hypoglycemia during 35 minutes only.

4.4 Conclusion and perspectives

This study shows that IL-1β-induced hypoglycemia is MyD88-dependent and paralleled by an increase in Lac/Cho, Cre/Cho and NAA/Cho ratios. One possible interpretation of these results is that, as opposed to the hypoglycemia caused by insulin, cerebral energy metabolism is increased during IL-1β-induced hypoglycemia. While performing the studies reported in this work, A. Löhrwald

showed that no changes in cerebral energy metabolism are detected in MyD88 KO mice, further indicating the involvement of MyD88-signalling in the mediation of IL-1β-induced hypoglycemia (Lörwald, 2012). It is clear, that further studies are needed to clarify the role of MyD88 in IL-1β-induced hypoglycemia. For example, it would be necessary to evaluate changes in the energy metabolism of hypothalamic, glucose-sensing neurons and its surrounding astrocytes. One approach would be to use *in vitro* cultures of cells obtained from WT and MyD88 KO mice.

Another aspect that needs detailed investigation to elucidate the mechanisms by which IL-1β changes glucose homeostasis at central levels, is to study if GLUT or monocarboxylate-transporter expression and incorporation into the cell membrane of neurons and astrocytes are affected by the cytokine.

Here, first evidence was provided that acute blockade of MyD88 leads to hyperglycaemia, which was further confirmed by A. Lörwald (Lörwald, 2012). Thus, the involvement of MyD88 in the physiological regulation of glucose homeostasis needs further investigation. *In vivo* experiments including i.c.v. injections of different antagonists of receptors that signal via MyD88 might help to identify the endogenous ligand that plays a role in basal glucose regulation. Furthermore, kinetics studies should be performed to investigate at what time after i.c.v. injection of IL-1β, maximal hypoglycemia is reached. So far it was only shown that IL-1β injected i.c.v. leads to hypoglycemia 4 h after injection (del Rey and Besedovsky, 1992).

How IL-1β leads to an increase in lactate remains to be elucidated by further *in vivo* and *in vitro* experiments. Due to resolution limits of the methodology used, we were only able to evaluate spectroscopically the whole brain. Thus, it would be important in future experiments to evaluate smaller, well-defined brain regions, such as the hypothalamus. Possible approaches are either enzymatic or HPLC determinations of glucose, lactate and ketone bodies in the hypothalamus or fluoro-2-desoxy-D-glucose positron emission tomography (FDG-PET) imaging. To further clarify the signalling mechanisms by which IL-1β activates the HPA-axis, experiments including i.c.v. injection of IL-1β in MyD88 KO mice and i.c.v. injection of MyD88 inhibitors into WT mice will be carried out in a following study.

Previous studies have shown that IL-1β is necessary for sustaining LTP, learning and memory, processes that are highly demanding in terms of energy

(Besedovsky and del Rey, 2011). This evidence, together with the results reported here showing that this cytokine changes brain energy metabolism, allow to hypothesise that IL-1 is needed to transfer energy substrates to activated neurons, as insulin does in peripheral tissues with high energetic needs. Besides its relevance for basic physiology, this might shed a new light on the role of IL-1 in neuropsychiatric diseases. So far, the research is focussed on the proinflammatory effects of IL-1 in neuropsychiatric diseases such as depression (Akhondzadeh et al., 2009; Dinan, 2009) or cognitive impairment (Gemma and Bickford, 2007). Since some of the symptoms of these diseases or even their aetiology might be explained by local or general impairments of cerebral energy metabolism, further investigation of the role of IL-1 in brain energy metabolism in pathologic conditions is needed.

5 References

ADACHI, O., KAWAI, T., TAKEDA, K., MATSUMOTO, M., TSUTSUI, H., SAKAGAMI, M., AKIRA, S. 1998. Targeted disruption of the MyD88 gene results in loss of IL-1- and IL-18-mediated. *Immunity, 9*(1), 143-150.

AGARDH, C. D., FOLBERGROVA, J., SIESJO, B. K. 1978. Cerebral metabolic changes in profound, insulin-induced hypoglycemia, and in the recovery period following glucose administration. *J Neurochem, 31*(5), 1135-1142.

AGWUNOBI, A. O., REID, C., MAYCOCK, P., LITTLE, R. A., CARLSON, G. L. 2000. Insulin resistance and substrate utilization in human endotoxemia. *J Clin Endocrinol Metab, 85*(10), 3770-3778.

AKHONDZADEH, S., JAFARI, S., RAISI, F., NASEHI, A. A., GHOREISHI, A., SALEHI, B., Kamalipour, A. 2009. Clinical trial of adjunctive celecoxib treatment in patients with major depression: a double blind and placebo controlled trial. *Depress Anxiety, 26*(7), 607-611.

AKIRA, S., TAKEDA, K. 2004. Toll-like receptor signalling. *Nat Rev Immunol* 4, 499-511.

ALLAN, S. M., TYRRELL, P. J., ROTHWELL, N. J. 2005. Interleukin-1 and neuronal injury. *Nat Rev Immunol* 5, 629-640.

ASHFORD, M. L., BODEN, P. R., TREHERNE, J. M. 1990. Glucose-induced excitation of hypothalamic neurones is mediated by ATP-sensitive K+ channels. *Pflugers Arch, 415*(4), 479-483.

ATKINS, E. 1960. Pathogenesis of fever. *Physiol Rev, 40*, 580-646.

AVITAL, A., GOSHEN, I., KAMSLER, A., SEGAL, M., IVERFELDT, K., RICHTER-LEVIN, G., YIRMIYA, R. 2003. Impaired interleukin-1 signaling is associated with deficits in hippocampal memory processes and neural plasticity. *Hippocampus, 13*(7), 826-834.

BACKENS, M. 2010. Basic principles of MR spectroscopy. *Radiologe, 50*(9), 767-774.

BANKS, W. A., FARR, S. A., MORLEY, J. E. 2002. Entry of blood-borne cytokines into the central nervous system: effects on cognitive processes. *Neuroimmunomodulation, 10*(6), 319-327.

BANKS, W. A., KASTIN, A. J. 1991. Blood to brain transport of interleukin links the immune and central nervous systems. *Life Sci, 48*(25), 117-121.

BANKS, W. A., KASTIN, A. J., DURHAM, D. A. 1989. Bidirectional transport of interleukin-1 alpha across the blood-brain barrier. *Brain Res Bull, 23*(6), 433-437.

BARKER, P. B., LIN, D. D. M. 2006. In vivo proton MR spectroscopy of the human brain. *Progress in Nuclear Magnetic Resonance Spectroscopy, 49*(2), 99-128.

BENDTZEN, K., MANDRUP-POULSEN, T., NERUP, J., NIELSEN, J. H., DINARELLO, C. A., SVENSON, M. 1986. Cytotoxicity of human interleukin-1 for pancreatic islets of Langerhans. *Science, 232*(4757), 1545-1547.

BERKENBOSCH, F., VAN OERS, J., DEL REY, A., TILDERS, F., BESEDOVSKY, H. 1987. Corticotropin-releasing factor-producing neurons in the rat activated by interleukin-1. *Science, 238*(4826), 524-526.

BESEDOVSKY, H.O., SORKIN, E., MUELLER J., 1975 Hormonal changes during the immune response*. Proc Soc Exp Biol 150*, 466-479.

BESEDOVSKY H.O., DEL REY A., SORKIN E., LOTZ W., SCHWULERA U. 1985 Lymphoid cells produce an immunoregulatory glucocorticoid increasing factor (GIF) acting through the pituitary gland*. Clin Exp Immunol. 59, 622-8.*

BESEDOVSKY, H., DEL REY, A. 1987. Neuroendocrine and metabolic responses induced by interleukin-1. *J Neurosci Res, 18*(1), 172-178.

BESEDOVSKY, H., DEL REY, A., SORKIN, E., DINARELLO, C. A. 1986. Immunoregulatory feedback between interleukin-1 and glucocorticoid hormones. *Science, 233*(4764), 652-654.

BESEDOVSKY, H. O., DEL REY, A. 1996. Immune-neuro-endocrine interactions: facts and hypotheses. *Endocr Rev, 17*(1), 64-102.

BESEDOVSKY, H. O., DEL REY., 2006 Regulating inflammation by glucocorticoids. *Nat. Immunol. 7(6):* 537

BESEDOVSKY, H. O., DEL REY, A. 2011. Central and peripheral cytokines mediate immune-brain connectivity. *Neurochem Res, 36*(1), 1-6.

BIRD, T. A., DAVIES, A., BALDWIN, S. A., SAKLATVALA, J. 1990. Interleukin 1 stimulates hexose transport in fibroblasts by increasing the expression of glucose transporters. *J Biol Chem, 265*(23), 13578-13583.

BITTSANSKY, M., VYBOHOVA, D., DOBROTA, D. 2012. Proton magnetic resonance spectroscopy and its diagnostically important metabolites in the brain. *Gen Physiol Biophys, 31*(1), 101-112.

BLOESCH, D., KELLER, U., SPINAS, G. A., KURY, D., GIRARD, J., STAUFFACHER, W. 1993. Effects of endotoxin on leucine and glucose kinetics in man: contribution of prostaglandin E2 assessed by a cyclooxygenase inhibitor. *J Clin Endocrinol Metab, 77*(5), 1156-1163.

BLUTHE, R. M., MICHAUD, B., KELLEY, K. W., DANTZER, R. (1996). Vagotomy attenuates behavioural effects of interleukin-1 injected peripherally but not centrally. *Neuroreport, 7*(9), 1485-1488.

BORG, M. A., SHERWIN, R. S., BORG, W. P., TAMBORLANE, W. V., SHULMAN, G. I. 1997. Local ventromedial hypothalamus glucose perfusion blocks counterregulation during systemic hypoglycemia in awake rats. *J Clin Invest, 99*(2), 361-365.

BORG, M. A., TAMBORLANE, W. V., SHULMAN, G. I., SHERWIN, R. S. 2003. Local lactate perfusion of the ventromedial hypothalamus suppresses hypoglycemic counterregulation. *Diabetes, 52*(3), 663-666.

BORG, W. P., DURING, M. J., SHERWIN, R. S., BORG, M. A., BRINES, M. L., SHULMAN, G. I. 1994. Ventromedial hypothalamic lesions in rats suppress counterregulatory responses to hypoglycemia. *J Clin Invest, 93*(4), 1677-1682.

BORG, W. P., SHERWIN, R. S., DURING, M. J., BORG, M. A., SHULMAN, G. I. 1995. Local ventromedial hypothalamus glucopenia triggers counterregulatory hormone release. *Diabetes, 44*(2), 180-184.

BROWN, A. M., RANSOM, B. R. 2007. Astrocyte glycogen and brain energy metabolism. *Glia, 55*(12), 1263-1271.

BROWN, A. M., SICKMANN, H. M., FOSGERAU, K., LUND, T. M., SCHOUSBOE, A., WAAGEPETERSEN, H. S., RANSOM, B. R. 2005. Astrocyte glycogen metabolism is required for neural activity during aglycemia or intense stimulation in mouse white matter. *J Neurosci Res, 79*(1-2).

BURDAKOV, D., LUCKMAN, S. M., VERKHRATSKY, A. 2005. Glucose-sensing neurons of the hypothalamus *Philos Trans R Soc Lond B Biol Sci,* 360, 2227-2235.

CAO, C., MATSUMURA, K., YAMAGATA, K., WATANABE, Y. 1997. Involvement of cyclooxygenase-2 in LPS-induced fever and regulation of its mRNA by LPS in the rat brain. *Am J Physiol,* 272, 1712-1725.

CHIH, C. P., LIPTON, P., ROBERTS, E. L., JR. 2001. Do active cerebral neurons really use lactate rather than glucose? *Trends Neurosci* 24, 573-578.

CLARK, J. B. 1998. N-acetyl aspartate: a marker for neuronal loss or mitochondrial dysfunction *Dev Neurosci,* 20, 271-276.

CONE, R. D., COWLEY, M. A., BUTLER, A. A., FAN, W., MARKS, D. L., LOW, M. J. 2001. The arcuate nucleus as a conduit for diverse signals relevant to energy homeostasis. *Int J Obes Relat Metab Disord, 25 Suppl 5*, 63-67.

CROWN, J., JAKUBOWSKI, A., KEMENY, N., GORDON, M., GASPARETTO, C., WONG, G., .ET AL. 1991. A phase I trial of recombinant human interleukin-1 beta alone and in combination. *Blood, 78*(6), 1420-1427.

DANTZER, R. 2009. Cytokine, sickness behavior, and depression *Immunol Allergy Clin North Am,* 29, 247-264.

DAVIS, C. N., MANN, E., BEHRENS, M. M., GAIDAROVA, S., REBEK, M., REBEK, J., JR., BARTFAI, T. 2006. MyD88-dependent and -independent signaling by IL-1 in neurons probed by bifunctional Toll/IL-1 receptor domain/BB-loop mimetics *Proc Natl Acad Sci,* 103, 2953-2958.

DE STEFANO, N., NARAYANAN, S., FRANCIS, G. S., ARNAOUTELIS, R., TARTAGLIA, M. C., ANTEL, J. P., ARNOLD, D. L. 2001. Evidence of axonal damage in the early stages of multiple sclerosis and its relevance to disability *Arch Neurol,* 58, 65-70.

DEL REY A., BESEDOVSKY H., SORKIN E., 1984. Endogenous blood levels of corticosterone control the immunologic cell mass and B cell activity in mice*. J Immunol. 133,* 572-5.

DEL REY, A., BESEDOVSKY, H. 1987. Interleukin 1 affects glucose homeostasis. *Am J Physiol,* 253, 794-798.

DEL REY, A., BESEDOVSKY, H. O. 1992. Metabolic and neuroendocrine effects of pro-inflammatory cytokines. *Eur J Clin Invest, 22 Suppl 1*, 10-15.

DEL REY, A., MONGE-ARDITI, G., BESEDOVSKY, H. O. 1998. Central and peripheral mechanisms contribute to the hypoglycemia induced by interleukin-1. *Ann N Y Acad Sci, 840*, 153-161.

DEL REY, A., ROGGERO, E., RANDOLF, A., MAHUAD, C., MCCANN, S., RETTORI, V., BESEDOVSKY, H. 2006. IL-1 resets glucose homeostasis at central levels. *Proc Natl Acad Sci, 103*(43), 16039-16044

DEL REY, A., BALSCHUN, D., WETZEL, W., RANDOLF, A., BESEDOVSKY, H. O. 2013. A cytokine network involving brain-borne IL-1β, IL-1ra, IL-18, IL-6, and TNFα operates during long-term potentiation and learning. *Brain Behav Immun, 33*, 15-23.

DIEM, R., HOBOM, M., GROTSCH, P., KRAMER, B., BAHR, M. 2003. Interleukin-1 beta protects neurons via the interleukin-1 (IL-1) receptor-mediated Akt pathway and by IL-1 receptor-independent decrease of transmembrane currents in vivo M*ol Cell Neurosci, 2*2, 487-500.

DILTOER, M., CAMU, F. 1988. Glucose homeostasis and insulin secretion during isoflurane anesthesia in humans. A*nesthesiology, 68(*6), 880-886.

DINAN, T. G. (2009). Inflammatory markers in depression. C*urr Opin Psychiatry, 22(*1), 32-36.

DINARELLO, C. A. (1991). Interleukin-1 and interleukin-1 antagonism. B*lood, 77(*8), 1627-1652.

DINARELLO, C. A. (1996). Biologic basis for interleukin-1 in disease. B*lood, 87(*6), 2095-2147.

DINARELLO, C. A. (2005). Interleukin-1beta C*rit Care Med,* 33, 460-462).

DINARELLO, C. A. (2010). IL-1: discoveries, controversies and future directions. E*ur J Immunol, 40(*3), 599-606.

DINARELLO, C. A. 2011. Interleukin-1 in the pathogenesis and treatment of inflammatory diseases B*lood* 117, 3720-3732.

EK, M., KUROSAWA, M., LUNDEBERG, T., ERICSSON, A. (1998). Activation of vagal afferents after intravenous injection of interleukin-1beta: role of endogenous prostaglandins. J *Neurosci, 18(*22), 9471-9479.

EVANS, M. L., MCCRIMMON, R. J., FLANAGAN, D. E., KESHAVARZ, T., FAN, X., MCNAY, E. C., SHERWIN, R. S. 2004. Hypothalamic ATP-sensitive K + channels play a key role in sensing hypoglycemia and triggering counterregulatory epinephrine and glucagon responses D*iabetes,* 53, 2542-2551.

FISCHEREDER, M., SCHROPPEL, B., WIESE, P., FINK, M., BANAS, B., SCHMIDBAUER, S., SCHLONDORFF, D. 2003. Regulation of glucose transporters in human peritoneal mesothelial cells. J *Nephrol, 16(*1), 103-109.

FOSCOLO, R. B., DE CASTRO, M. G., MARUBAYASHI, U., DOS REIS, A. M., COIMBRA, C. C. 2003. Medial preoptic area adrenergic receptors modulate glycemia and insulinemia in freely moving rats. B*rain Res, 985(*1), 56-64.

FUJIMOTO, K., BOSNJAK, Z. J., KWOK, W. M. (2002). Isoflurane-induced facilitation of the cardiac sarcolemmal K(ATP) channel A*nesthesiology,* 97, 57-65).

FUKUZUMI, M., SHINOMIYA, H., SHIMIZU, Y., OHISHI, K., UTSUMI, S. 1996. Endotoxin-induced enhancement of glucose influx into murine peritoneal macrophages via GLUT1. I*nfect Immun, 64(*1), 108-112.

GARCIA-LEME, J., FARSKY, S. P. 1993. Hormonal control of inflammatory responses. M*ediators Inflamm, 2(*3), 181-198.

GARCIA-WELSH, A., SCHNEIDERMAN, J. S., BALY, D. L. 1990. Interleukin-1 stimulates glucose transport in rat adipose cells. Evidence for receptor discrimination between IL-1 beta and IL-1 alpha. *FEBS Lett*, 269, 421-424.

GARLANDA, C., DINARELLO C.A., MANTOVANI A. 2013. The interleukin-1 family: back to the future. *Immunity,* 39(6), 1003-18.

GEMMA, C., BICKFORD, P. C. 2007. Interleukin-1beta and caspase-1: players in the regulation of age-related cognitive dysfunction. *Rev Neurosci, 18(*2), 137-148.

GIBERTINI, M., NEWTON, C., FRIEDMAN, H., KLEIN, T. W. 1995. Spatial learning impairment in mice infected with Legionella pneumophila or administered exogenous interleukin-1-beta B*rain Behav Immun,* 9, 113-128.

GOSSELIN, D., BELLAVANCE, M. A., RIVEST, S. 2013. IL-1RAcPb signaling regulates adaptive mechanisms in neurons that promote their long-term survival following excitotoxic insults. *Front Cell Neurosci, 7,* 9.

GOSSELIN, D., RIVEST, S. 2008. MyD88 signaling in brain endothelial cells is essential for the neuronal activity and glucocorticoid release during systemic inflammation. *Mol Psychiatry, 13(*5), 480-497.

GOULD, G. W., CUENDA, A., THOMSON, F. J., COHEN, P. 1995. The activation of distinct mitogen-activated protein kinase cascades is required for the stimulation of 2-deoxyglucose uptake by interleukin-1 and insulin-like growth factor-1 in KB cells. *Biochem J*, 311(3), 735-738.

HAYAKAWA, K., ARAI, K., LO, E. H. 2010. Role of ERK map kinase and CRM1 in IL-1beta-stimulated release of HMGB1 from cortical astrocytes. G*lia, 58(*8), 1007-1015.

HOSOI, T., YOKOYAMA, S., MATSUO, S., AKIRA, S., OZAWA, K. 2010. Myeloid differentiation factor 88 (MyD88)-deficiency increases risk of diabetes in mice. *PLoS One, 5(*9).

HUANG, Y., SMITH, D. E., IBANEZ-SANDOVAL, O., SIMS, J. E., FRIEDMAN, W. J. 2011. Neuron-specific effects of interleukin-1beta are mediated by a novel isoform of. *J Neurosci, 31(*49), 18048-18059.

KABIERSCH, A., DEL REY, A., HONEGGER, C. G., BESEDOVSKY, H. O. 1988. Interleukin-1 induces changes in norepinephrine metabolism in the rat brain. *Brain Behav Immun, 2(*3), 267-274.

KAWAI, T., ADACHI, O., OGAWA, T., TAKEDA, K., AKIRA, S. 1999. Unresponsiveness of MyD88-deficient mice to endotoxin *Immunity,* 11, 115-122.

KENNY, E. F., O'NEILL, L. A. 2008. Signalling adaptors used by Toll-like receptors: an update. *Cytokine, 43(*3), 342-349.

KOH, Y. S., KOO, J. E., BISWAS, A., KOBAYASHI, K. S. 201). MyD88-dependent signaling contributes to host defense against ehrlichial infection. *PLoS One, 5(*7).

KOL, S., BEN-SHLOMO, I., RUUTIAINEN, K., ANDO, M., DAVIES-HILL, T. M., ROHAN, R. M., .ADASHI, E. Y. 1997. The midcycle increase in ovarian glucose uptake is associated with enhanced expression of glucose transporter 3. Possible role for interleukin-1, a putative intermediary in the ovulatory process. *J Clin Invest, 99(*9), 2274-2283.

KONSMAN, J. P., PARNET, P., DANTZER, R. (2002). Cytokine-induced sickness behaviour: mechanisms and implications. *Trends Neurosci,* 25, 154-159.

LATTERMANN, R., WACHTER, U., GEORGIEFF, M., GOERTZ, A., SCHRICKER, T. 2003. Catabolic stress response during and after abdominal surgery. Comparison between two anaesthesia procedures. *Anaesthesist, 52(*6), 500-506.

LEADBETTER, E. A., RIFKIN, I. R., HOHLBAUM, A. M., BEAUDETTE, B. C., SHLOMCHIK, M. J., MARSHAK-ROTHSTEIN, A. 2002. Chromatin-IgG complexes activate B cells by dual engagement of IgM and Toll-like receptors. *Nature, 416(*6881), 603-607.

LEIBOWITZ, S. F. 1988. Hypothalamic paraventricular nucleus: interaction between alpha 2-noradrenergic system and circulating hormones and nutrients in relation to energy balance. *Neurosci Biobehav Rev, 12(*2), 101-109.

LEWIS, L. D., LJUNGGREN, B., NORBERG, K., SIESJO, B. K. 1974. Changes in carbohydrate substrates, amino acids and ammonia in the brain during insulin-induced hypoglycemia. *J Neurochem, 23(*4), 659-671.

LOIARRO, M., SETTE, C., GALLO, G., CIACCI, A., FANTO, N., MASTROIANNI, D., RUGGIERO, V. 2005. Peptide-mediated interference of TIR domain dimerization in MyD88 inhibits interleukin-1-dependent activation of NF-{kappa}B. *J Biol Chem, 280(*16), 15809-15814.

LOVATT, D., SONNEWALD, U., WAAGEPETERSEN, H. S., SCHOUSBOE, A., HE, W., LIN, J. H., NEDERGAARD, M. 2007. The transcriptome and metabolic gene signature of protoplasmic astrocytes in the adult murine cortex *J Neurosci,* 27, 12255-12266.

LÖRWALD, A. 2012. Involvement of the MyD88-signalling pathway in the brain on IL-1β-induced hypoglyemia*. Diploma Thesis, Philipps-Universität, Marburg*.

LYNCH, M.A. 2004. Long-Term Potentiation and Memory. *Physiol Rev,* 84, 87-134

MANGIA, S., DINUZZO, M., GIOVE, F., CARRUTHERS, A., SIMPSON, I. A., VANNUCCI, S. J. 2011. Response to 'comment on recent modeling studies of astrocyte-neuron metabolic interactions': much ado about nothing *J Cereb Blood Flow Metab,* 31, 1346-1353.

MATOUSEK, S. B., GHOSH, S., SHAFTEL, S. S., KYRKANIDES, S., OLSCHOWKA, J. A., O'BANION, M. K. 2012. Chronic IL-1beta-mediated neuroinflammation mitigates amyloid pathology in a mouse model of Alzheimer's disease without inducing overt neurodegeneration. *J Neuroimmune Pharmacol, 7(*1), 156-164.

MCCRIMMON, R. J., EVANS, M. L., FAN, X., MCNAY, E. C., CHAN, O., DING, Y., SHERWIN, R. S. 2005. Activation of ATP-sensitive K+ channels in the ventromedial hypothalamus amplifies counterregulatory hormone responses to hypoglycemia in normal and recurrently hypoglycemic rats. *Diabetes*, 54, 3169-3174.

MCCUSKER, R.H., KELLEY, K.W., 2013. Immune-neural connections: how the immune system's response to infectious agents influences behaviour. *J Exp Biol,* 216(1), 84–98

MERBOLDT, K. D., BRUHN, H., HANICKE, W., MICHAELIS, T., FRAHM, J. 1992. Decrease of glucose in the human visual cortex during photic stimulation. *Magn Reson Med, 25(*1), 187-194.

METZGER, S., NUSAIR, S., PLANER, D., BARASH, V., PAPPO, O., SHILYANSKY, J., CHAJEK-SHAUL, T. 2004. Inhibition of hepatic gluconeogenesis and enhanced glucose uptake contribute to the development of hypoglycemia in mice bearing interleukin-1beta- secreting tumor *Endocrinology* 145, 5150-5156.

MOFFETT, J. R., ROSS, B., ARUN, P., MADHAVARAO, C. N., NAMBOODIRI, A. M. 2007. N-Acetylaspartate in the CNS: from neurodiagnostics to neurobiology. *Prog Neurobiol, 81(*2), 89-131.

O'NEILL, L. A., BOWIE, A. G. (2007). The family of five: TIR-domain-containing adaptors in Toll-like receptor signalling. *Nat Rev Immunol, 7(*5), 353-364.

ODA, K., KITANO, H. 2006. A comprehensive map of the toll-like receptor signaling network. *Mol Syst Biol, 2,* 15

OGIMOTO, K., HARRIS, M. K., JR., WISSE, B. E. 2006. MyD88 is a key mediator of anorexia, but not weight loss, induced by lipopolysaccharide and interleukin-1 beta. *Endocrinology, 147(*9), 4445-4453.

OOMURA, Y., ONO, T., OOYAMA, H., WAYNER, M. J. 1969. Glucose and osmosensitive neurones of the rat hypothalamus. *Nature, 222(*5190), 282-284.

Ota, K., WILDMANN, J., OTA, T., BESEDOVSKY, H., DEL REY, A. 2009. Interleukin-1beta and insulin elicit different neuroendocrine responses to hypoglycemia. *Ann N Y Acad Sci,* 1153, 82-88.

PARKER, L. C., LUHESHI, G. N., ROTHWELL, N. J., PINTEAUX, E. 2002. IL-1 beta signalling in glial cells in wildtype and IL-1RI deficient mice. *Br J Pharmacol, 136(2*), 312-320.

PARSADANIANTZ, S. M., LEBEAU, A., DUVAL, P., GRIMALDI, B., TERLAIN, B., KERDELHUE, B. 2000. Effects of the inhibition of cyclo-oxygenase 1 or 2 or 5-lipoxygenase on the activation of the hypothalamic-pituitary-adrenal axis induced by interleukin-1beta in the male Rat. *J Neuroendocrinol,* 12, 766-773.

PELLERIN, L. 2008. Brain energetics (thought needs food). *Curr Opin Clin Nutr Metab Care, 11(6*), 701-705.

PELLERIN, L., MAGISTRETTI, P. J. 1994. Glutamate uptake into astrocytes stimulates aerobic glycolysis: a mechanism. *Proc Natl Acad Sci, 91(2*2), 10625-10629.

PLATA-SALAMAN, C. R., FFRENCH-MULLEN, J. M. 1992. Intracerebroventricular administration of a specific IL-1 receptor antagonist blocks

food and water intake suppression induced by interleukin-1 beta. *Physiol Behav, 51(6*), 1277-1279.

PRICHARD, J., ROTHMAN, D., NOVOTNY, E., PETROFF, O., KUWABARA, T., AVISON, M., SHULMAN, R. 1991. Lactate rise detected by 1H NMR in human visual cortex during physiologic stimulation. *Proc Natl Acad Sci U S A, 88(1*3), 5829-5831.

RACHAL PUGH, C., FLESHNER, M., WATKINS, L. R., MAIER, S. F., RUDY, J. W. 2001. The immune system and memory consolidation: a role for the cytokine IL-1beta. *Neurosci Biobehav Rev,* 25, 29-41.

RAETZSCH, C. F., BROOKS, N. L., ALDERMAN, J. M., MOORE, K. S., HOSICK, P. A., KLEBANOV, S., COMBS, T. P. 2009. Lipopolysaccharide inhibition of glucose production through the Toll-like receptor-4, myeloid differentiation factor 88, and nuclear factor kappa b pathway. *Hepatology, 50(2*), 592-600.

RAO, R., ENNIS, K., LONG, J. D., UGURBIL, K., GRUETTER, R., TKAC, I. 2010. Neurochemical changes in the developing rat hippocampus during prolonged hypoglycemia. *J Neurochem, 114(3*), 728-738.

RITTER, S., DINH, T. T., LI, A. J. 2006. Hindbrain catecholamine neurons control multiple glucoregulatory responses. *Physiol Behav, 89(4*), 490-500.

RUPP, E. A., CAMERON, P. M., RANAWAT, C. S., SCHMIDT, J. A., BAYNE, E. K. 1986. Specific bioactivities of monocyte-derived interleukin 1 alpha and interleukin 1 beta are similar to each other on cultured murine thymocytes and on cultured human connective tissue cells. *J Clin Invest, 78(3*), 836-839.

SAKURAI, T. (2007). The neural circuit of orexin (hypocretin): maintaining sleep and wakefulness. *Nat Rev Neurosci,* 8, 171-181.

SAPOLSKY, R., RIVIER, C., YAMAMOTO, G., PLOTSKY, P., VALE, W. 1987. Interleukin-1 stimulates the secretion of hypothalamic corticotropin-releasing factor. *Science, 238(4*826), 522-524.

SAPPEY-MARINIER, D., CALABRESE, G., FEIN, G., HUGG, J. W., BIGGINS, C., WEINER, M. W. 1992. Effect of photic stimulation on human visual cortex lactate and phosphates using 1H and 31P magnetic resonance spectroscopy. *J Cereb Blood Flow Metab, 12(4*), 584-592.

SCANGA, C. A., ALIBERTI, J., JANKOVIC, D., TILLOY, F., BENNOUNA, S., DENKERS, E. Y., SHER, A. 2002. Cutting edge: MyD88 is required for resistance to Toxoplasma gondii infection and regulates parasite-induced IL-12 production by dendritic cells. *J Immunol, 168(12*), 5997-6001.

SCHNEIDER, H., PITOSSI, F., BALSCHUN, D., WAGNER, A., DEL REY, A., BESEDOVSKY, H. O. 1998. A neuromodulatory role of interleukin-1beta in the hippocampus. *Proc Natl Acad Sci, 95(1*3), 7778-7783.

SCHRICKER, T., GALEONE, M., WYKES, L., CARLI, F. 2004. Effect of desflurane/remifentanil anaesthesia on glucose metabolism during surgery: a

comparison with desflurane/epidural anaesthesia. *Acta Anaesthesiol Scand,* 48, 169-173.

SCHWARCZ, A., NATT, O., WATANABE, T., BORETIUS, S., FRAHM, J., MICHAELIS, T. 2003. Localized proton MRS of cerebral metabolite profiles in different mouse strains. *Magn Reson Med, 49(5*), 822-827.

SEINO, S., MIKI, T. 2003. Physiological and pathophysiological roles of ATP-sensitive K+ channels. *Prog Biophys Mol Biol,* 81, 133-176.

SHERWIN, R. S. 2008. Bringing light to the dark side of insulin: a journey across the blood-brain. *Diabetes,* 57, 2259-2268.

SHIKHMAN, A. R., BRINSON, D. C., VALBRACHT, J., LOTZ, M. K. 2001 Cytokine regulation of facilitated glucose transport in human articular chondrocytes. *J Immunol*, 167, 7001-7008.

SHIKHMAN, A. R., BRINSON, D. C., LOTZ, M. K. 2004. Distinct pathways regulate facilitated glucose transport in human articular. *Am J Physiol Endocrinol Metab, 286(6*), E980-985.

SIMPSON, I. A., DWYER, D., MALIDE, D., MOLEY, K. H., TRAVIS, A., VANNUCCI, S. J. 2008. The facilitative glucose transporter GLUT3: 20 years of distinction. *Am J Physiol Endocrinol Metab,* 295, E242-253.

SIMS, J. E., SMITH, D. E. 2010. The IL-1 family: regulators of immunity. *Nat Rev Immunol, 10(2*), 89-102.

SMITH, J. W., LONGO, D. L., ALVORD, W. G., JANIK, J. E., SHARFMAN, W. H., GAUSE, B. L. 1993. The effects of treatment with interleukin-1 alpha on platelet recovery after high-dose carboplatin. N *Engl J Med, 328(1*1), 756-761.

SOARES, D. P., LAW, M. 2009. Magnetic resonance spectroscopy of the brain: review of and clinical applications. *Clin Radiol, 64(1*), 12-21.

SONG, Z., ROUTH, V. H. 2005. Differential effects of glucose and lactate on glucosensing neurons in the ventromedial hypothalamic nucleus. Di*abetes,* 54, 15-22).

STYLIANOU, E., O'NEILL, L. A., RAWLINSON, L., EDBROOKE, M. R., WOO, P., SAKLATVALA, J. 1992. Interleukin 1 induces NF-kappa B through its type I but not its type II receptor in lymphocytes. *J Biol Chem, 267(2*2), 15836-15841.

SUH, S. W., BERGHER, J. P., ANDERSON, C. M., TREADWAY, J. L., FOSGERAU, K., SWANSON, R. A. (2007). Astrocyte glycogen sustains neuronal activity during hypoglycemia: studies with the glycogen phosphorylase inhibitor CP-316,819 ([R-R*,S*]-5-chloro-N-[2-hydroxy-3-(methoxymethylamino)-3-oxo-1-(phenylmethyl)pro pyl]-1H-indole-2-carboxamide). *J Pharmacol Exp Ther, 321(1*), 45-50.

SUTHERLAND, G. R., TYSON, R. L., AUER, R. N. 2008. Truncation of the krebs cycle during hypoglycemic coma. *Med Chem, 4(4*), 379-385.

TAKEUCHI, O., HOSHINO, K., AKIRA, S. 2000. Cutting edge: TLR2-deficient and MyD88-deficient mice are highly susceptible to Staphylococcus aureus infection. *J Immunol, 165(1*0), 5392-5396.

TANAKA, K., KAWANO, T., NAKAMURA, A., NAZARI, H., KAWAHITO, S., OSHITA, S., NAKAYA, Y. 2007. Isoflurane activates sarcolemmal adenosine triphosphate-sensitive potassium channels in vascular smooth muscle cells: a role for protein kinase A. *Anesthesiology,* 106, 984-991.

TANAKA, K., KAWANO, T., TSUTSUMI, Y. M., KINOSHITA, M., KAKUTA, N., HIROSE, K., OSHITA, S. 2011. Differential effects of propofol and isoflurane on glucose utilization and insulin secretion. *Life Sci,* 88, 96-103.

TSAKIRI, N., KIMBER, I., ROTHWELL, N. J., PINTEAUX, E. 2008. Interleukin-1-induced interleukin-6 synthesis is mediated by the neutral sphingomyelinase/Src kinase pathway in neurones. *Br J Pharmacol,* 153, 775-783.

TURNBULL, A. V., RIVIER, C. L. 1999. Regulation of the hypothalamic-pituitary-adrenal axis by cytokines: actions and mechanisms of action. *Physiol Rev, 79(1*), 1-71.

VAN TASSELL, B. W., SEROPIAN, I. M., TOLDO, S., SALLOUM, F. N., SMITHSON, L., VARMA, A., ABBATE, A. 2010. Pharmacologic inhibition of myeloid differentiation factor 88 (MyD88) prevents left ventricular dilation and hypertrophy after experimental acute myocardial infarction in the mouse. *J Cardiovasc Pharmacol, 55(4*), 385-390.

VANNUCCI, S. J., MAHER, F., SIMPSON, I. A. 1997. Glucose transporter proteins in brain: delivery of glucose to neurons and glia. *Glia,* 21, 2-21.

VEGA, C., PELLERIN, L., DANTZER, R., MAGISTRETTI, P. J. 2002. Long-term modulation of glucose utilization by IL-1 alpha and TNF-alpha in astrocytes: Na+ pump activity as a potential target via distinct signaling mechanisms. *Glia, 39(1*), 10-18.

VIVIANI, B., BARTESAGHI, S., GARDONI, F., VEZZANI, A., BEHRENS, M. M., BARTFAI, T., MARINOVICH, M. 2003. Interleukin-1beta enhances NMDA receptor-mediated intracellular calcium increase through activation of the Src family of kinases. *J Neurosci,* 23, 8692-8700.

WALLIMANN, T., WYSS, M., BRDICZKA, D., NICOLAY, K., EPPENBERGER, H. M. 1992. Intracellular compartmentation, structure and function of creatine kinase isoenzymes in tissues with high and fluctuating energy demands: the 'phosphocreatine circuit' for cellular energy homeostasis. *Biochem J, 281 (*1), 21-40.

WEBER, A., WASILIEW, P., KRACHT, M. 2010. Interleukin-1 (IL-1) pathway. Sc*i Signal, 3(1*05).

WEISHAUPT, D., KÖCHLI, V. D., MARINCEK, B. 2009. Wie *funktioniert MRI?* Springer Berlin Heidelberg.

WYSS, M., KADDURAH-DAOUK, R. 2000. Creatine and creatinine metabolism. Ph*ysiol Rev, 80(3*), 1107-1213.

YIRMIYA, R., WINOCUR, G., GOSHEN, I. 2002. Brain interleukin-1 is involved in spatial memory and passive avoidance conditioning. *Neurobiol Learn Mem,* 78, 379-389.

ZEN, M., CANOVA, M., CAMPANA, C., BETTIO, S., NALOTTO, L., RAMPUDDA, M., RAMONDA, R., IACCARINO, L., DORIA, A. 2011. The kaleidoscope of glucocorticoid effects on immune system. *Autoimmun Rev 10 (6):* 305-310

ZHOU, S., KURT-JONES, E. A., MANDELL, L., CERNY, A., CHAN, M., GOLENBOCK, D. T., FINBERG, R. W. 2005. MyD88 is critical for the development of innate and adaptive immunity during acute lymphocytic choriomeningitis virus infection. *Eur J Immunol, 35(3*), 822-830.

6 APPENDIX

Verzeichnis der akademischen LehrerInnen

Meine akademischen LehrerInnen waren die Damen / Herren

Aigner	Hasilik	Plant
Aumüller	Hertl	Preisig – Müller
Barth	Hofmann	Rausch
Basler	Hoyer	Renz
Bauer	Klose	Richter
Baum	Koolman	Röhm
Behr	Lill	Röper
Berger	Löffler	Rothmund
Bien	Lohoff	Ruchholtz
Cetin	Maisch	Schäfer
Czubayko	Moll	Schade
Daut	Mueller	Schneider
Dietrich	Mutters	Schulze
Engenhard-Cabillic	Neubauer	Seitz
Feuser	Neumüller	Steiniger
Fuchs - Winkelmann	Nimsky	Voigt
Grzeschik	Oertel	Vogelmaier
Gress	Pagenstecher	Weihe
Grundmann	Hasilik	Werner

Danksagung

Prof. Dr. Adriana del Rey und Prof. Dr. Hugo Besedovsky danke ich für die Überlassung des Themas dieser Arbeit und die ausgezeichneten Möglichkeiten es zu bearbeiten. Ich fand bei beiden stets ein offenes Ohr und die Möglichkeit vorläufige Ergebnisse kritisch zu diskutieren und weitere Schritte zu planen. Von unschätzbarem Wert waren die Vorschläge und Anregungen, mit denen mir Beide beim Verfassen der Dissertation zur Seite standen. Ebenso danke ich Andrea Lörwald, Dr. Johannes Wildmann und Dr. Anke Randolf, die mir während der Durchführung der Experimente mit Rat und Tat zur Seite standen. Auch

Alexander König, Maximilian Völker und Steven Braun gilt mein Dank. Ohne sie wären die MRS-Experimente nicht möglich gewesen. Des Weiteren danke ich Marion Vogel, Dr. Jan Verdenhalven und Nicolas Brune für die Korrektur von Rechtschreib- und Grammatikfehlern.

Veröffentlichung von Teilen der vorliegenden Arbeit

Ko-Autorenschaft bei einer Publikation, die kürzlich zur Veröffentlichung eingereicht wurde